Rapid and strain-specific resistance evolution of *Staphylococcus aureus* against inhibitory molecules secreted by *Pseudomonas aeruginosa*

Selina Niggli[1*], Lucy Poveda[2], Jonas Grossmann[2], Rolf Kümmerli[1**]

[1] Department of Quantitative Biomedicine, University of Zurich, Winterthurerstrasse 190, 8057 Zurich, Switzerland

[2] Functional Genomics Center Zurich, ETH Zurich and University of Zurich, Winterthurerstrasse 190, 8057 Zurich, Switzerland

Corresponding authors:

* selina.niggli@uzh.ch

** rolf.kuemmerli@uzh.ch

Abstract

Pseudomonas aeruginosa and *Staphylococcus aureus* frequently occur together in polymicrobial infections, and there is evidence that their interactions negatively affect disease outcome in patients. At the molecular level, interactions between the two bacterial taxa are well-described, with *P. aeruginosa* usually being the dominant species suppressing *S. aureus* through a variety of inhibitory molecules. However, in polymicrobial infections, the two species interact over prolonged periods of time, and *S. aureus* might evolve resistance against inhibitory molecules deployed by *P. aeruginosa*. Here, we used experimental evolution to test this hypothesis by exposing three different *S. aureus* strains (Cowan I, 6850, JE2) to the growth-inhibitory supernatant of *P. aeruginosa* PAO1 over 30 days. We found that all three *S. aureus* strains rapidly evolved resistance against inhibitory molecules and show that (i) adaptations were strain-specific; (ii) resistance evolution affected the expression of virulence traits; and (iii) mutations in membrane transporters were the most frequent evolutionary targets. Our work indicates that adaptations of *S. aureus* to co-infecting pathogens could increase virulence and decrease antibiotic susceptibility, because both virulence traits and membrane transporters involved in drug resistance were under selection. Thus, pathogen co-evolution could exacerbate infections and compromise treatment options.

Introduction

Bacterial infections are frequently caused by multiple species (Brogden, Guthmiller, and Taylor 2005; Peters et al. 2012) and such polymicrobial infections can be more severe than the respective mono-species infections (Jorge et al. 2018; Lim, Lim, and Ray 2013; Pammi et al. 2014; Tan et al. 2016). Because of the detrimental effects for patients, there is high interest in understanding the mechanisms of bacterial interactions and how they affect ecological dynamics between co-infecting species. Interactions between the two opportunistic human pathogens *Pseudomonas aeruginosa* (PA) and *Staphylococcus aureus* (SA) have attracted particularly high attention (Hotterbeekx et al. 2017; Limoli and Hoffman 2019). This is because they are major pathogens and often co-occur in the lungs of cystic fibrosis (CF) patients, and in burn and chronic wound infections (Dowd et al. 2008; Gjødsbøl et al. 2006; Hubert et al. 2013; Maliniak, Stecenko, and McCarty 2016). Co-infections with PA and SA can be associated with more severe disease outcomes in humans (Gangell et al. 2011; Maliniak, Stecenko, and McCarty 2016), and studies in animal models confirmed increased virulence and compromised antibiotic treatment options during co-infections (Dalton et al. 2011; Hendricks et al. 2001; Pastar et al. 2013).

Laboratory studies established a solid mechanistic understanding of how the two species interact, and generally agree that the relationship between PA and SA is antagonistic (Filkins et al. 2015; Niggli and Kümmerli 2020; Yung, Sircombe, and Pletzer 2021). Overall, PA seems to dominate the interactions through the production and secretion of a variety of inhibitory molecules, such as the staphylolytic protease LasA, siderophores, and the respiratory chain inhibitors HQNO and phenazines (Harrison et al. 2008; Hoffman et al. 2006; Kessler et al. 1993; Lin et al. 2018; Mashburn et al. 2005; Soberón-Chávez, Lépine, and Déziel 2005). There is also increasing knowledge on ecological factors that influence interactions patterns. For example, during early childhood, CF lungs are often first colonized by SA followed by PA later on, with SA abundance tending to decrease when PA increases (Nguyen and Oglesby-Sherrouse 2016). In the context of wound infections, we also have an increased

58 understanding about the spatial localization of the two species, where it seems that PA and
59 SA occupy different niches (Fazli et al. 2009; Phalak et al. 2016).

60 In contrast to these mechanistic and ecological insights, we know little about whether
61 interactions between PA and SA can evolve. Species co-evolution is likely to occur in chronic
62 infections, where pathogens repeatedly interact, and is predicted to alter disease parameters
63 and treatment strategies. In the context of interactions between PA and SA, we hypothesize
64 that SA could adapt and become resistant to PA inhibitory molecules. Such adaptation could
65 in turn foster co-existence of the two species, potentially contribute to the clinically observed
66 higher virulence, increased morbidity and treatment complications (Gangell et al. 2011;
67 Maliniak, Stecenko, and McCarty 2016).

68 Here, we test our hypothesis by using a combination of experimental evolution,
69 phenotypic screening, and whole-genome sequencing of evolved clones. Specifically, we first
70 conducted a series of experiments with three different clinical SA strains to show that all of
71 them are inhibited by a secreted compound regulated by the PQS quorum-sensing system in
72 the supernatant of the PA standard laboratory strain PAO1. We then exposed the three SA
73 strains to either the PA supernatant (containing inhibitory molecules, mixed with fresh medium)
74 or regular medium only (as a control) for 30 consecutive days, by transferring evolving cultures
75 every 48 hours to fresh PA supernatant or regular medium. Following experimental evolution,
76 we isolated evolved SA clones from replicated populations to screen them for resistance
77 phenotypes and to explore whether virulence traits were under selection. Finally, we
78 sequenced the whole genome of 150 clones to determine the genetic basis of SA resistance
79 evolution against inhibitory molecules produced by PA.

80

81 **Results**

82 **Growth of SA strains is reduced in the presence of PA supernatant**

83 Previous work showed that PA can inhibit SA via a diverse set of secreted molecules, including
84 proteases, biosurfactants, siderophores, and toxic compounds (Hotterbeekx et al. 2017). To
85 test whether our three SA strains (Cowan I, 6850 and JE2, Table S1) are also inhibited by PA,

86 we exposed them to the sterile-filtered supernatant of PA PAO1, harvested from overnight
87 cultures (30% supernatant in 70% fresh tryptic soy broth, TSB). We found that all three SA
88 strains were negatively affected by the PA supernatant compared to growth under control
89 condition (30% NaCl in 70% TSB, Figure 1). Exposure to PA supernatant significantly reduced
90 overall growth performance (Figure S1a, ANOVA on growth integrals followed by Tukey's HSD
91 pairwise comparisons: $p_{adj} < 0.0001$ for all SA strains), and specifically extended the lag phase
92 of all SA strains (Figure S1b). We also observed SA strain-specific responses (Figure 1).
93 Cowan I featured an intermediate extension of the lag phase (10.3 hours compared to 6.6
94 hours in the control medium), a premature stationary phase, followed by a decrease in OD_{600}
95 possibly indicating cell death. 6850 suffered from an extremely long lag phase extension (19.7
96 hours vs. 6.9 hours), also showed a premature growth stop, but no OD_{600} decline. JE2 was
97 least affected by the PA supernatant. Its lag phase extension was not as pronounced (8.4 hours
98 vs. 5.6 hours), and it grew steadily afterwards, albeit to a lower yield than the control.

99 We also conducted the reciprocal experiments by exposing PA to the supernatants of
100 the three SA strains, but found no inhibition (Figure S2). Taken together, our supernatant
101 assays reveal unilateral inhibition: PA produces inhibitory molecules that negatively affect the
102 growth of genetically different SA strains.

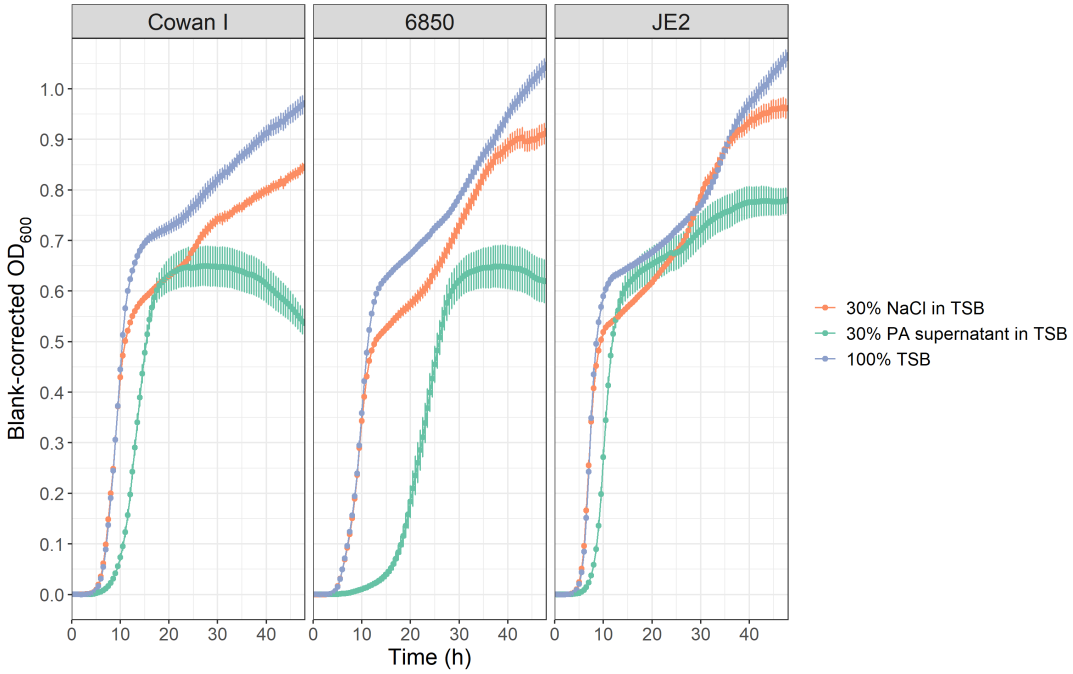

103

104 **Figure 1.** Supernatant of PA inhibits growth of three different SA strains (Cowan I, 6850, JE2). Growth
105 trajectories of SA strains were followed over 48 hours at 37 °C under three different conditions: 30%
106 NaCl in TSB (control 1), 30% PA supernatant in TSB (experimental treatment) and 100% TSB (control
107 2). Curves show the average growth (± standard error) across seven independent experiments and a
108 total of 28 replicates per strain and condition. See Figure S1 for a statistical comparison of growth
109 parameters extracted from these curves.
110

111 **The PQS pathway is involved in compromising SA growth**

112 To identify possible PA pathways or traits involved in the inhibition of SA, we screened a small
113 panel of seven PA candidate mutants and checked whether the inhibitory effects of their
114 supernatants towards SA were altered. We found one hit: the supernatant of PAO1*ΔpqsA* did
115 no longer inhibit SA (Table 1, Figure S3).
116

117 **Table 1.** Relative effects of supernatants from wildtype and mutant *P. aeruginosa* (PA) strains on *S.*
118 *aureus* (SA) growth.

PA supernatant donor strain	Phenotype of mutant strain	Relative growth* of Cowan I in PA supernatant	Relative growth* of 6850 in PA supernatant	Relative growth* of JE2 in PA supernatant
PAO1 wild type	wild type	0.78 (± 0.20)	0.60 (± 0.23)	0.87 (± 0.18)
MPAO1 wild type	wild type	0.75 (± 0.23)	0.59 (± 0.21)	0.72 (± 0.18)
PAO1*ΔlasR*	Las quorum sensing signal blind	0.34 (± 0.08)	0.38 (± 0.10)	0.50 (± 0.19)
PAO1*ΔrhlI*	Rhl quorum sensing signal negative	0.65 (± 0.05)	0.45 (± 0.11)	0.67 (± 0.05)
PAO1*ΔrhlR*	Rhl quorum sensing signal blind	0.70 (± 0.13)	0.60 (± 0.05)	0.70 (± 0.03)
PAO1*ΔrhlA*	Rhamnolipid null mutant	0.61 (± 0.11)	0.54 (± 0.15)	0.68 (± 0.07)
MPAO1*ΔpqsA*	Alkylquinolone null mutant	**1.22 (± 0.16)**	**1.22 (± 0.10)**	**1.05 (± 0.12)**
PAO1*ΔpvdDΔpchEF*	Siderophore null mutant	0.63 (± 0.01)	0.23 (± 0.04)	0.68 (± 0.02)
PAO1*ΔlecA*	Lectin null mutant	0.67 (± 0.02)	0.42 (± 0.01)	0.83 (± 0.06)

119

120 *The relative supernatant effect (± standard deviation) is expressed as the growth integral of SA over
121 48 hours in 30% PA supernatant + TSB divided by the growth integral of SA in 30% NaCl + TSB.
122 Values < 1 indicate growth inhibition, while values > 1 (in bold) indicate cases with no inhibition.
123

124 PqsA is an anthranilate-coenzyme A ligase that plays a role in PA cell-to-cell
125 communication (quorum sensing) (Dubern and Diggle 2008). It is directly involved in the

synthesis of a family of secondary metabolites, including 4-hydroxy-2-heptylquinoline (HHQ), 2-n-heptyl-4-hydroxyquinoline N-oxide (HQNO) and the *Pseudomonas* quinolone signal (PQS). HHQ, HQNO and PQS have previously been suggested to be inhibitory against a variety of bacterial and fungal species (Hoffman et al. 2006; Orazi and O'Toole 2017; Ramos et al. 2020; Toyofuku et al. 2010). Here, we tested whether they also inhibit our SA strains by focusing on PQS as one of the molecules synthetized by PqsA. We exposed all three SA strains to increasing concentrations of synthetic PQS and found a dose-dependent reduction in growth (Figure 2). This indicates that PQS is involved in the SA growth inhibition that we observed in our supernatant assays.

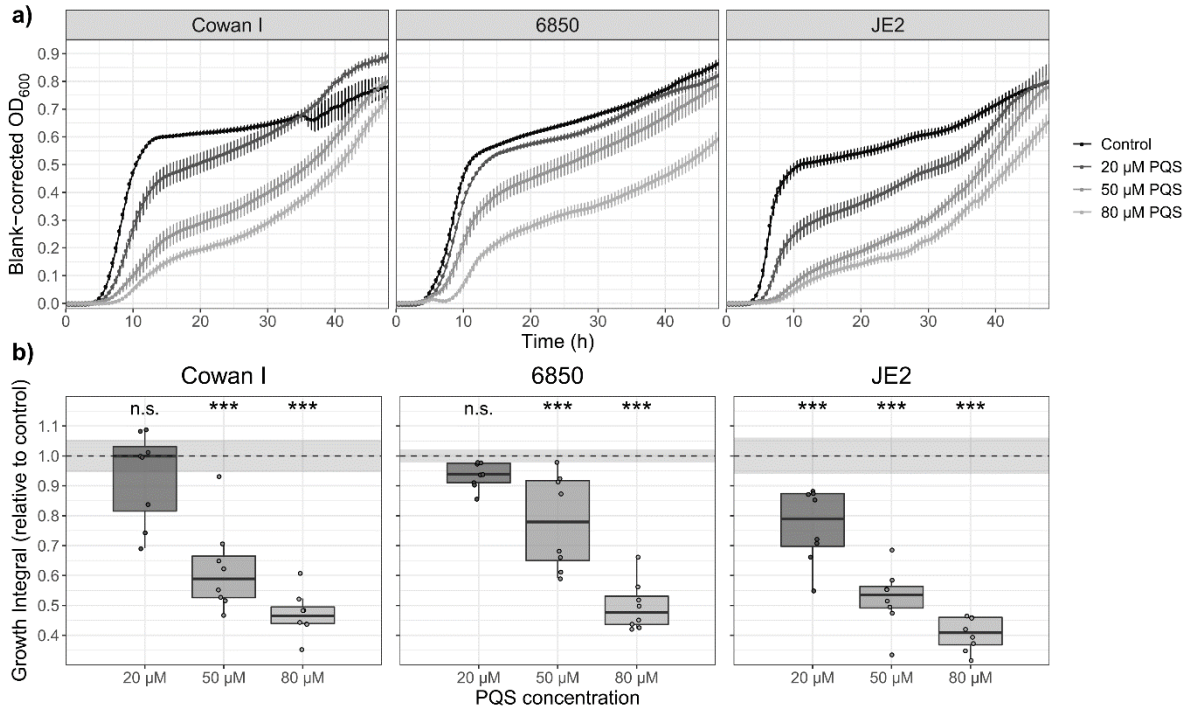

Figure 2. Synthetic PQS suppresses the growth of all three SA strains. SA strains Cowan I, 6850 and JE2 were grown in the presence of increasing concentrations of PQS (20 µM, 50 µM, 80 µM) and OD_{600} was recorded over 48 hours at 37 °C. As a control, we used TSB containing the same volume of DMSO as the 80 µM PQS condition (labelled as 'control', black). (a) Growth trajectories of the three different SA strains in the presence of increasing concentrations of PQS, shown as means ± standard errors. (b) Integrals over the growth trajectories of the three SA strains, relative to the control (dotted line at 1.0 ± 95% confidence interval depicted as shaded area). Box plots show the median (bold line), the first and third quartiles, and the 1.5* inter-quartile range (IQR, whiskers) or the range from the lowest to highest value if all values fall within the 1.5* IQR. Asterisks denote significant differences from the control as determined by Tukey's HSD. *** $p < 0.001$; n.s. not significant. Data are from two independent experiments with eight replicates in total per SA strain and condition.

147 **All SA strains evolve resistance to PA supernatant inhibition**

148 We then asked whether SA can adapt to the PA-induced growth inhibition. This is conceivable
149 because the PA supernatant shows anti-bacterial activity, and one could expect SA to evolve
150 resistance against this activity, in similar ways as pathogens evolve resistance against
151 clinically administered antibiotics. To address this question, we performed an experimental
152 evolution experiment, during which we exposed the three SA strains to either 30% PA
153 supernatant in 70% TSB or to 100% TSB over 30 days, in seven-fold replication (Figure S4).
154 Every 48 hours, we transferred evolving cultures into fresh medium (30% PA supernatant in
155 TSB or 100% TSB) using a 1:10,000 dilution. After experimental evolution, we quantified the
156 growth of evolved populations and randomly isolated evolved clones (five clones per replicate
157 = 210 clones in total) in both experimental media.

158 We found that populations that had evolved in the presence of PA supernatant showed
159 significantly improved growth performance compared to their respective ancestors when
160 exposed to the PA supernatant, indicating the evolution of resistance (Figure 3a, Cowan I: t_{12}
161 = 11.41, $p < 0.0001$; 6850: $t_{12} = 6.31$, $p = 0.0002$; JE2: $t_{12} = 3.61$, $p = 0.0072$). Conversely, all
162 populations that evolved in 100% TSB were still fully or even more susceptible to the PA
163 supernatant compared to the ancestor (Figure 3a, Cowan I: $t_{12} = -3.98$, $p = 0.0055$; 6850: t_{12} =
164 1.00, $p = 0.4039$; JE2: $t_{12} = -0.87$, $p = 0.4368$). Next, we tested whether evolved populations
165 showed TSB-specific adaptations. In support of this view, we found that populations of Cowan
166 I and JE2 that evolved in 100% TSB significantly increased their growth in this medium, but
167 not 6850 (Figure 3b, Cowan I: $t_{12} = 11.09$, $p < 0.0001$; 6850: $t_{12} = -0.77$, $p = 0.4590$; JE2: t_{12} =
168 3.70, $p = 0.0072$). In contrast, populations of all three SA strains that evolved in the presence
169 of PA supernatant did not show improved growth in TSB (Figure 3b, Cowan I: $t_{12} = 2.32$, p =
170 0.0663; 6850: $t_{12} = 1.41$, $p = 0.2467$; JE2: $t_{12} = 1.94$, $p = 0.1137$). These results show that all
171 three SA strains have specifically adapted to the presence of PA supernatant and not merely
172 to TSB, and that these adaptations nullify the growth inhibition originally imposed by the PA
173 supernatant.

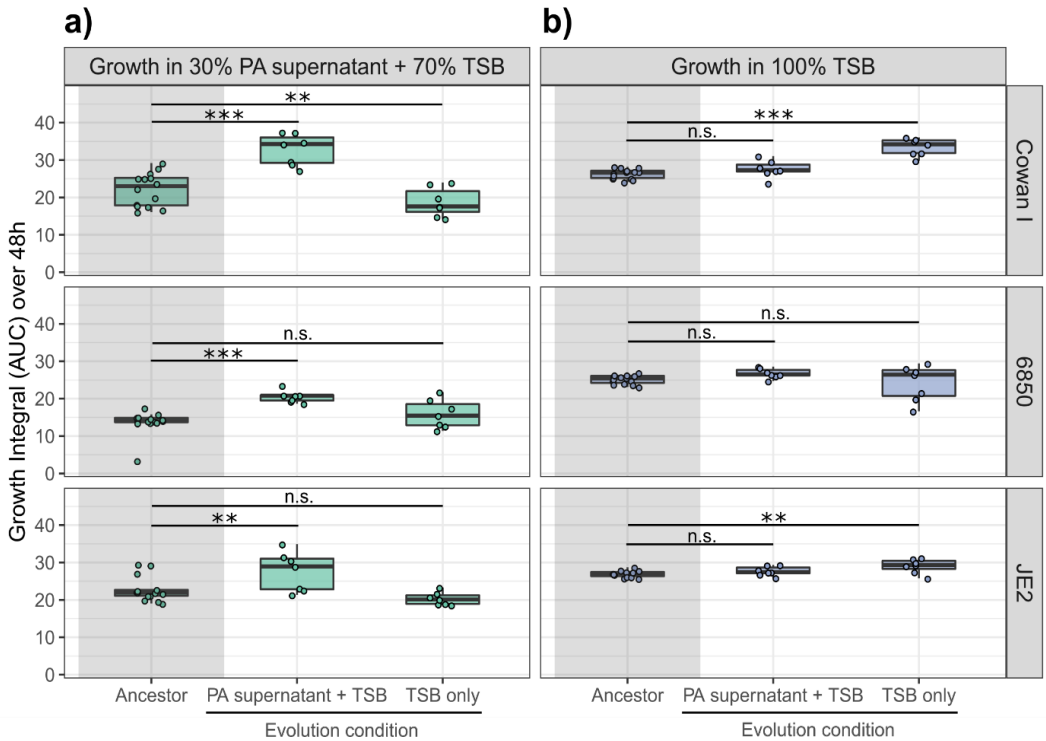

Figure 3. All three SA strains (Cowan I, 6850 and JE2) evolved resistance to inhibitory molecules produced by PA when exposed to its supernatant during experimental evolution (measured as growth integrals over 48 hours, area under the curve). Populations of SA strains either evolved in 30% PA supernatant + 70% TSB or 100% TSB over 30 days with transfer to fresh medium every 48 hours. a) Growth of ancestral (grey-shaded area) and evolved populations in medium containing 30% PA supernatant + 70% TSB. SA populations evolved in the presence of PA supernatant significantly improved growth, while populations evolved in TSB alone are still inhibited by the supernatant. b) Growth of ancestral (grey-shaded area) and evolved populations in 100% TSB medium. SA populations evolved in the presence of PA supernatant did not improve growth in TSB alone, while populations evolved in TSB did so for two of the three SA strains. Box plots show the median (bold line), the first and third quartiles, and the 1.5* inter-quartile range (IQR, whiskers) or the range from the lowest to highest value if all values fall within the 1.5* IQR. Asterisks denote significant differences between the ancestral and evolved populations. *** $p < 0.001$; ** $p < 0.01$; n.s. not significant. P-values are adjusted by the false discovery rate method.

We then repeated all the above growth assays with the 210 individual clones. The results confirmed our population-level analysis (Figure S5). Overall, we observed considerable variation among clones in their growth phenotype. This suggests that populations are heterogenous, consisting of multiple different genotypes, an aspect we confirm in our phenotypic and genomic analyses below.

196 **Clones evolved in the presence of PA supernatant overproduce staphyloxanthin (STX)**

197 From an infection perspective, it is important to understand whether adaptation to a competitor
198 involves traits that also affect the host and could have consequences for virulence. We
199 therefore screened our collection of evolved clones for changes in phenotypes, which we
200 anticipated to be involved in resistance evolution towards PA supernatant and are known to
201 have virulence consequences. We restricted our analysis to 150 clones from 30 out of the 42
202 populations, as this sample size matched our genomic sequencing contingent.

203 At first, we quantified the production of staphyloxanthin (STX), the golden carotenoid
204 pigment. STX acts as an antioxidant and virulence factor (Clauditz et al. 2006), and could be
205 under selection in the presence of PA (Antonic et al. 2013). We found that STX production
206 changed during the course of evolution (Figure 4a) and was significantly higher in clones that
207 evolved in the presence of PA supernatant than in clones evolved in TSB alone (ANOVA: $F_{1,146}$
208 $= 16.37$, $p < 0.0001$). Moreover, there were significant differences between SA strains ($F_{2,146} =$
209 22.93, $p < 0.0001$). While all clones of 6850 and JE2 that evolved in PA supernatant had
210 increased STX production compared to the ancestor, the same was true only for a fraction of
211 Cowan I clones. In TSB alone, evolved clones from Cowan I even showed decreased STX
212 production relative to the ancestor, whereas many of the evolved 6850 clones (and some JE2
213 clones) also increased STX production under this evolution condition. These analyses show
214 that STX production is generally under selection in TSB but reaches particularly high levels in
215 the presence of PA supernatant.

216

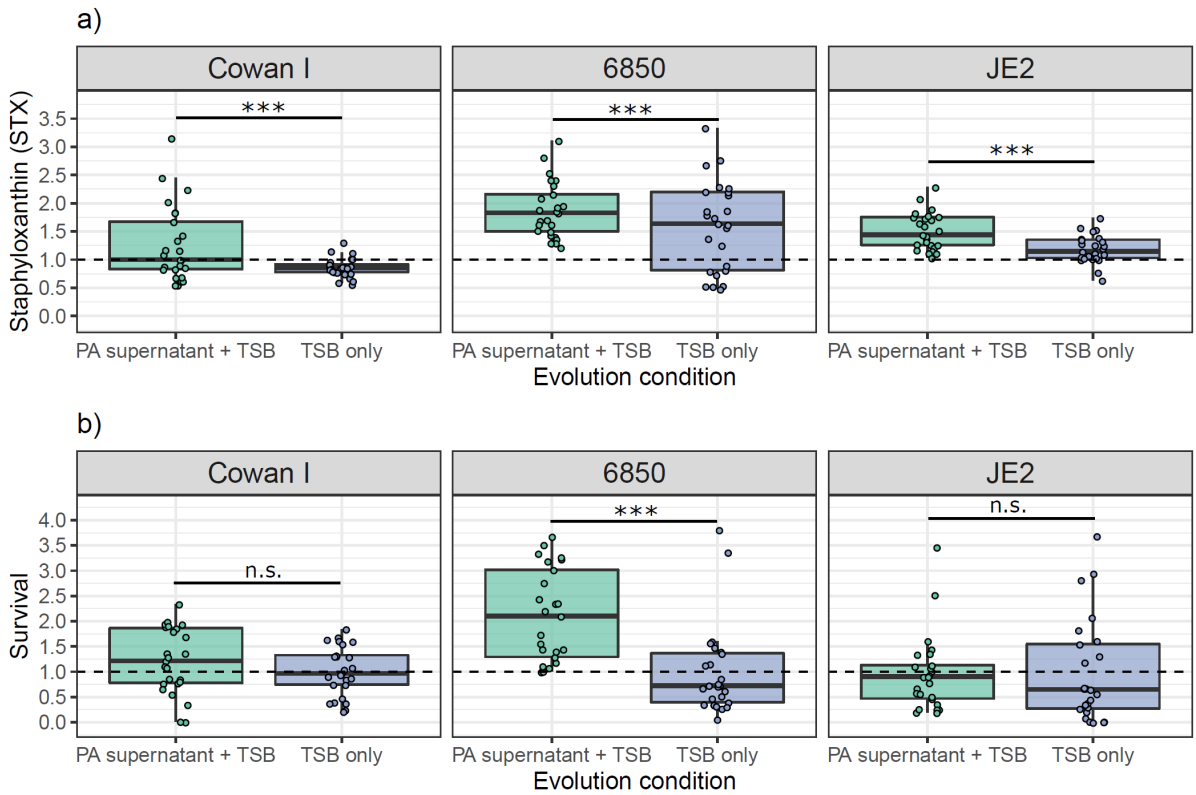

Figure 4. Change in staphyloxanthin (STX) production and survival in the presence of hydrogen peroxide (H_2O_2) during experimental evolution varies across SA strains and between media conditions. a) Production of STX for evolved clones from Cowan I, 6850 and JE2, expressed relative to the respective ancestor (dashed line at 1.0). STX was assessed by measuring the absorbance of the crude extract containing STX for 150 evolved clones (25 clones from 5 populations per strain and condition) at λ = 465 nm. b) Survival of evolved clones from Cowan I, 6850 and JE2 after exposure for one hour to 1.5% H_2O_2, expressed relative to the respective ancestor (dashed line at 1.0). Survival was measured as the number of colony forming units on TSB + 1.2% agar plates relative to an unchallenged control for the same 150 clones. Every dot represents the average value from two independent STX extractions and survival assays per clone. Box plots show the median (bold line), the first and third quartiles, and the 1.5* inter-quartile range (IQR, whiskers) or the range from the lowest to highest value if all values fall within the 1.5* IQR. Asterisks denote significant differences between the two evolution conditions for each SA strain (Tukey's HSD with adjusted p-values). *** $p < 0.001$; n.s. not significant.

Adaptation towards oxidative stress is SA strain specific

Inhibitory molecules from the PQS system can cause oxidative stress in target cells (Abdalla et al. 2017; Bredenbruch et al. 2006; Tognon et al. 2019) and we therefore wondered whether clones that evolved in the presence of PA supernatant are more resistant towards oxidative stress. Thus, we exposed all clones and the respective ancestors for one hour to a 1.5%

237 hydrogen peroxide (H_2O_2) solution and determined their survival compared to the unstressed
238 control. We observed that the survival of evolved SA clones depended on a significant
239 interaction between strain background and experimental medium (ANOVA: $F_{2,144} = 6.81$, $p =$
240 0.0015, Figure 4b). This interaction is driven by 6850, as for this strain clones evolved in the
241 presence of PA supernatant survived significantly better than clones evolved in TSB alone. No
242 such significant treatment effects were observed for Cowan I and JE2 clones.

243 Since the carotenoid pigment STX is involved in protection against reactive oxygen
244 species (Xue et al. 2019), we tested whether clones with increased STX production showed
245 higher survival in the presence of H_2O_2. Indeed, we found a positive correlation between STX
246 production and survival for clones evolved in the presence of PA supernatant (Pearson's
247 product-moment correlation, $r_{73} = 0.27$, $p = 0.0207$, Figure S6a), but not for clones evolved in
248 TSB alone ($r_{73} = -0.02$, $p = 0.8920$, Figure S6b). In sum, the survival data highlights that the
249 three SA strains differ in their adaptation towards PA supernatant and that evolved clones of
250 6850 showed the highest improvements in both STX production and survival rate.

251

252 **Formation of small colony variants in the presence of PA supernatant**

253 As small colony variants (SCVs) offer protection from stressful conditions, including reactive
254 oxygen species (Biswas et al. 2009; Hoffman et al. 2006; Kahl, Becker, and Löffler 2016;
255 Tuchscherr et al. 2011), we anticipated increased SCV formation to be another evolutionary
256 response of SA towards inhibitory molecules produced by PA. Consequently, we tested
257 whether SCV frequency increased during experimental evolution. Screening for SCVs is
258 difficult, as colony size is a variable trait and phenotypic unstable SCVs can quickly revert back
259 to regular colony sizes (Leimer et al. 2016). Our first screen involved the plating of evolved
260 populations on agar plates to detect the presence of SCVs. We found SCVs in five out of seven
261 Cowan I populations that had evolved in the presence of PA supernatant (Figure S7). SCVs
262 also surfaced in populations of other strains and media, but at a reduced rate (Cowan I in TSB
263 [2 out of 7 populations]; 6850 in TSB [1/7]; JE2 in PA supernatant + TSB [1/7]).

264 The above screen suggests that SCV formation occurs most commonly in Cowan I in
265 response to PA supernatant exposure. For this reason, we screened all evolved clones from
266 this evolution condition and found that five out of the 25 Cowan I clones expressed a SCV
267 phenotype. We classified three and two of these clones as dynamic/unstable and stable SCVs,
268 respectively. Dynamic/unstable SCVs consistently formed two colony types (small and normal-
269 sized colonies) upon repeated re-streaking. When comparing their growth trajectories in PA
270 supernatant + TSB to the Cowan I ancestor, they had a shorter lag phase and a higher yield
271 (Figure 5a). The two stable SCVs had a longer lag phase and a lower yield than the normal-
272 sized clones isolated from the same population. However, the death phase observed in the
273 Cowan I ancestor was abrogated, suggesting that stable SCV formation increases survival
274 under stressful conditions (Figure 5b). From these analyses, we conclude that both
275 dynamic/unstable and stable SCV formation can be adaptive strategies. While the former
276 increases overall growth performance, the latter prevents cell death at high population density.
277

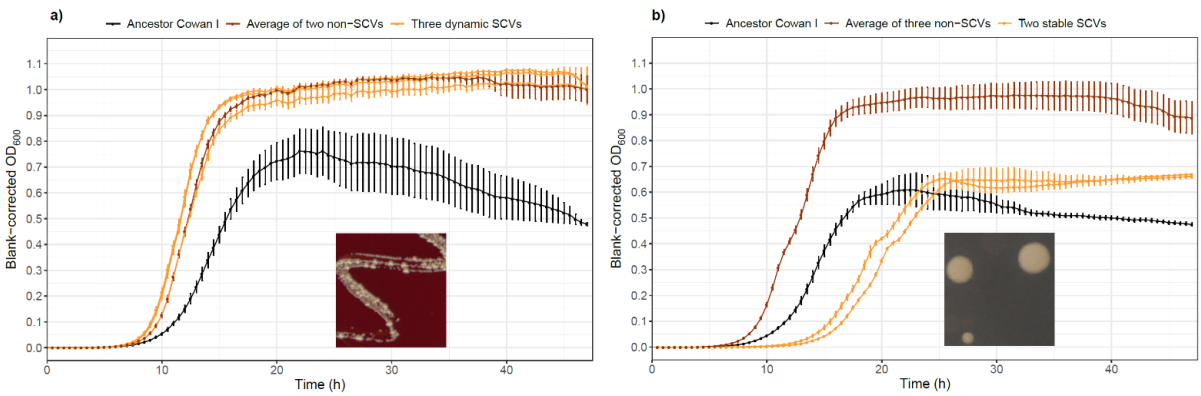

278 **Figure 5.** Characteristics of the five small colony variants (SCVs) evolved in the Cowan I background.
279 a) Growth trajectories of the three dynamic/unstable SCVs in 30% PA supernatant + 70% TSB.
280 Compared to the Cowan I ancestor, dynamic/unstable SCVs have a shorter lag phase and a higher
281 yield, which is similar to the normal-sized clones isolated from the same population. The inset shows
282 one of the dynamic/unstable SCVs with the two colony types on a sheep blood agar plate. b) Growth
283 trajectories of stable SCVs in 30% PA supernatant + 70% TSB. Compared to normal-sized clones from
284 the same population, the two stable SCVs have a longer lag phase and a lower growth yield, but they
285 no longer show the decrease in OD_{600} that is characteristic for the Cowan I ancestor. The inset shows a
286 stable SCV (bottom-left) compared to two normal-sized colonies (upper left and right) from the
287 population from which the two stable SCVs were isolated. Curves show the average growth (± standard
288 error) across 4 replicates.

289 **The presence of PA supernatant maintains hemolysis**

290 Hemolysis (lysis of red blood cells) is an important virulence-related phenotype in SA, and its
291 expression is regulated in complex ways, including the accessory gene regulator (agr) system
292 and other regulatory genes (Burnside et al. 2010). The loss of hemolysis has repeatedly been
293 observed in SA isolates from chronic infections (Shopsin et al. 2008; Traber et al. 2008).

294 Here, we asked whether the presence of PA supernatant affects the evolution of this
295 phenotype in 6850 and JE2 (Cowan I is a non-hemolytic SA strain, due to partial agr
296 dysfunctionality). Our population (Figure S8) and clonal (Figure 6) level analysis show that the
297 majority of 6850 and JE2 clones and populations remained hemolytic after evolution in PA
298 supernatant + TSB. In contrast, after evolution in 100% TSB, hemolytic activity only remained
299 high in clones from 6850 (72% still showed ancestral activity, Figure 6a), while 84% of the JE2
300 clones lost their hemolytic activity (Figure 6b), a pattern that was also reflected at the
301 population level (Figure S8). These findings show that the presence of PA supernatant fosters
302 the maintenance of hemolysis, and that the speed by which hemolysis can be lost depends on
303 the SA strain genetic background.

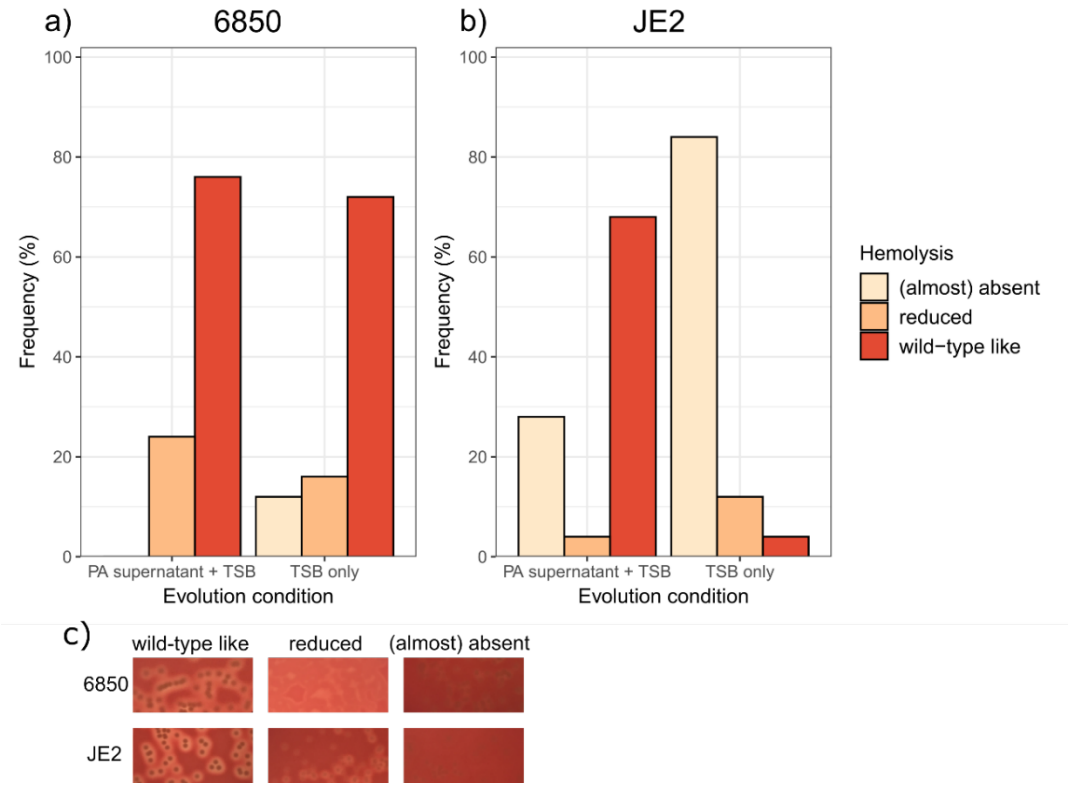

304

305 **Figure 6.** The PA supernatant selects for the maintenance of hemolysis in JE2. 100 evolved clones
306 were plated on sheep blood agar plates to score their hemolysis levels according to three categories:
307 wild-type like (ancestral), reduced, (almost) absent. Note that the Cowan I ancestor is non-hemolytic
308 and therefore not part of this assay. a) Frequency of the three hemolysis categories for the evolved 6850
309 clones. There is no significant difference in the hemolysis profiles between clones evolved in PA
310 supernatant + TSB versus in TSB only (Fisher's exact test: $p = 0.2266$) and most clones remained
311 hemolytic. b) Frequency of the three hemolysis categories for the evolved JE2 clones. There is a
312 significant difference in the hemolysis profiles between clones evolved in PA supernatant + TSB versus
313 in TSB only (Fisher's exact test: $p < 0.0001$). The large majority of JE2 clones evolved in TSB only are
314 no longer hemolytic. c) Representative pictures of the three hemolysis categories for the SA strains
315 6850 and JE2.
316

317 **SA strains follow divergent and medium-specific evolutionary trajectories**

318 We performed a principal component analysis (PCA) to statistically test whether the observed
319 phenotypic changes are SA strain background and/or media specific. The following four
320 phenotypes of 150 evolved clones were integrated into the PCA: (i) growth in 100% TSB; (ii)
321 growth in 30% PA supernatant + 70% TSB; (iii) STX production; and (iv) survival in the
322 presence of oxidative stress. We found that evolved clones significantly clustered based on
323 the evolution condition (PERMANOVA; $F_{1,144} = 36.59$, $p = 0.0010$, Figure 7), strain background
324 ($F_{2,144} = 24.06$, $p = 0.0010$), and their interaction ($F_{2,144} = 11.79$, $p = 0.0010$). The PCA therefore
325 clearly supports our notion that evolutionary trajectories differ across SA strain background
326 and media.

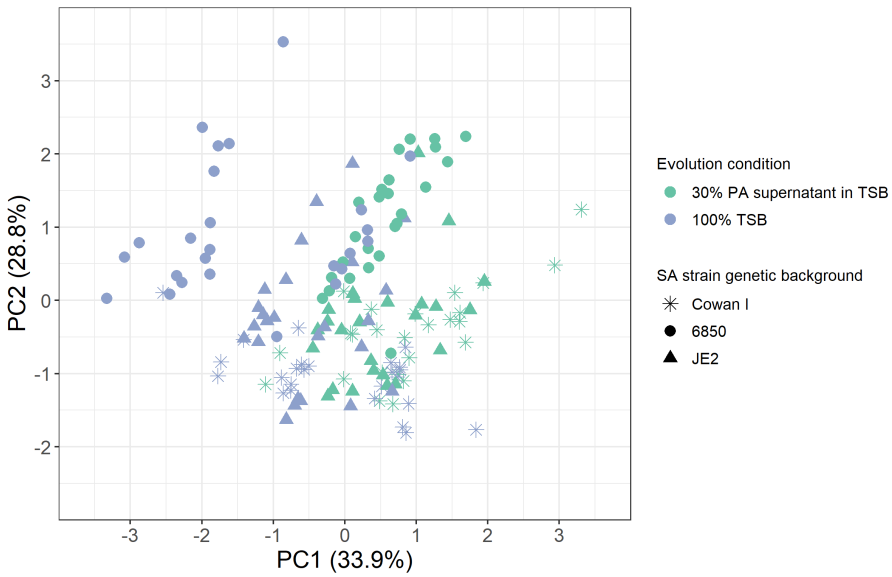

327

328 **Figure 7.** Principal component analysis (PCA) on the phenotypes of 150 evolved clones reveals strain
329 and media specific evolutionary divergence. The following four phenotypes were integrated into the
330 PCA: growth in 30% PA supernatant + 70% TSB, growth in 100% TSB, staphyloxanthin production and
331 survival in the presence of oxidative stress. The first two principal components (PC1 and PC2) explain
332 62.7% of the total variance in the data set. Statistical analyses reveal significant divergences in the
333 evolved phenotypes between the three SA strains (Cowan, 6850, JE2), and the condition they evolved
334 in (30% PA supernatant + 70% TSB, 100% TSB).
335

336 **Mutational patterns of evolved clones are media-specific**

337 To identify the genetic basis of the observed evolutionary changes, we sequenced the genome
338 of all the 150 evolved clones for which we collected the above phenotypes, and the three SA
339 ancestors Cowan I, 6850 and JE2. Compared to the ancestors, we identified nonsynonymous
340 mutations in 119 different genes and mutations in 51 different intergenic regions across all
341 evolved clones. Among those, 68 and 109 genes or intergenic regions were mutated in clones
342 that had evolved in PA supernatant + TSB and in 100% TSB, respectively. The large majority
343 (96.6%) of the 119 genes with nonsynonymous mutations occurred uniquely in one of the two
344 media (either in PA supernatant + TSB or 100% TSB), and there was little overlap in mutational
345 targets between strains (Figure 8a). These results are in line with our phenotypic assays,
346 highlighting that each SA strain followed a divergent evolutionary trajectory in each of the two
347 media.

348 For all three SA strains, the median number of mutations was lower for clones evolved
349 in PA supernatant + TSB than in 100% TSB (Cowan I: 2.0 vs. 4.0; 6850: 1.0 vs. 4.0; JE2: 2.0
350 vs. 5.0, Figure 8b), indicating that fewer mutations were beneficial in the presence of PA
351 supernatant than in TSB alone. The ratio of nonsynonymous to synonymous SNPs (dN/dS)
352 was higher than one for all strains and in both media (dN/dS for Cowan I: PA supernatant +
353 TSB / 100% TSB = 3.1 / 2.5; for 6850: 13.0 / 12.0; for JE2 3.6 / 4.0). These results show that
354 positive selection and adaptive evolution occurred in both conditions.

355 To determine whether the mutational patterns differed between the two media and the
356 three SA strains in terms of the functional classes affected, we sorted the mutated genes using
357 aureowiki (Fuchs et al. 2018) and the primary literature. Indeed, in clones that evolved in the

358 presence of PA supernatant, we found an enrichment of mutated genes belonging to the
359 category ‘membrane transporter’, while for clones that had evolved in TSB alone, most
360 mutated genes belonged to the categories ‘metabolism’, ‘cell wall organization’ and ‘signal
361 transduction’ (Figure 8c).

362

a)

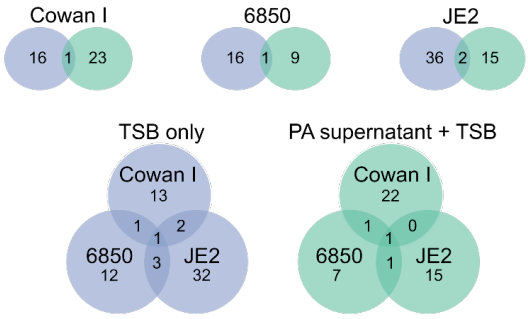

b)

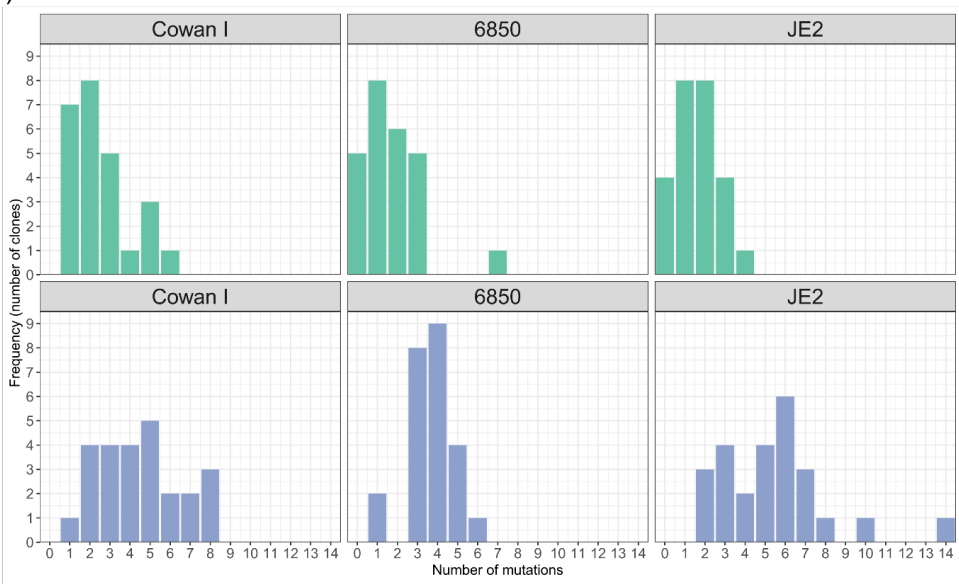

c)

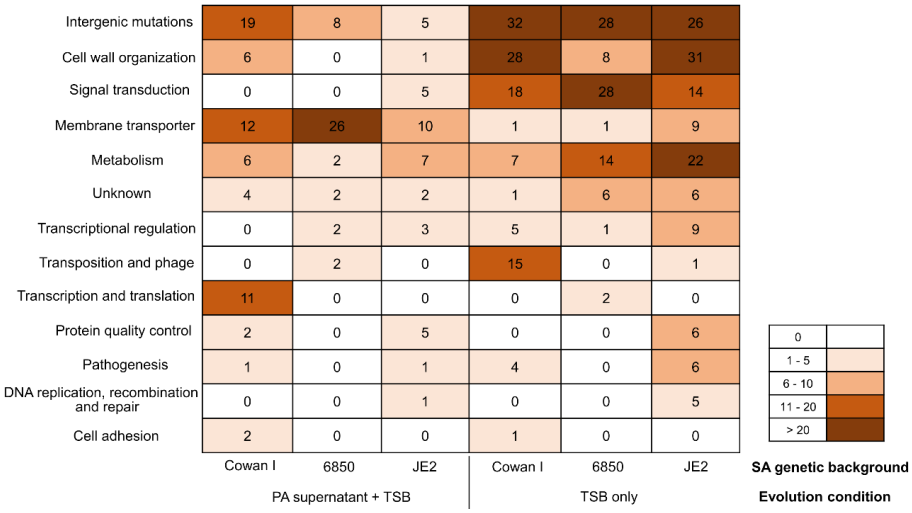

363

364 **Figure 8.** Genomic analysis of 150 evolved clones reveals strain and media specific mutational patterns.
365 a) Venn diagrams showing how often genes with nonsynonymous mutations are unique to or shared
366 between evolution conditions (top row) and the three SA ancestors (bottom row). There is little overlap
367 among mutated genes, indicating that most mutations are unique to the specific evolution condition and
368 SA strain. b) Number of mutations per clone (nonsynonymous and intergenic mutations) split according
369 to SA strain background (Cowan I, 6850, JE2) and evolution condition (green: 30% PA supernatant +
370 70% TSB; blue: 100% TSB). Clones evolved in the presence of PA supernatant had significantly fewer
371 mutations than clones evolved in TSB alone. c) Heatmap showing the total abundance of mutations in
372 functional gene categories and intergenic regions (top row) across all sequenced clones, split by SA
373 strain background (Cowan I, 6850, JE2) and evolution condition (30% PA supernatant + 70% TSB or
374 100% TSB). Note that we counted every mutation in every clone for this latter analysis.
375

376 **Parallel evolution in TSB, diverse non-parallel evolution in PA supernatant**

377 Next, we explored whether there is evidence for parallel evolution, which should manifest in
378 similar mutational patterns surfacing across independently evolved populations and strains.
379 For this purpose, we identified genes that mutated more than once in at least two
380 populations/strains. Across both evolution conditions, we found 11 genes that fulfilled these
381 criteria (Table S2). When focusing on the TSB alone medium, there were three genes (*fmtA*,
382 *gdpP*, *walK*) that stood out in terms of both their frequency of mutations and distribution across
383 SA strains. The teichoic acid D-Ala esterase *fmtA* mutated in five Cowan I populations, one
384 6850 population, and five JE2 populations [5/1/5]. Mutations in the cyclic-di-AMP
385 phosphodiesterase *gdpP* [0/4/5] and the cell wall histidine kinase *walK* [5/3/0] were similarly
386 frequent. A striking pattern is that mutations in any of these three genes are only common in
387 two out of the three SA strains in changing combinations. These results demonstrate that (i)
388 there is high level of parallel evolution between populations of the same strain; (ii) there is a
389 certain level of parallel evolution across strains but the combination of genes that are under
390 selection varies; and (iii) mutations in *fmtA*, *gdpP* and *walK* are likely involved in general
391 adaptations to the TSB medium, as these genes are not under selection in the PA supernatant
392 treatment.

393 For populations evolved in PA supernatant + TSB, we found a different pattern. Only
394 the gene *alsT* mutated in all SA strain backgrounds (Cowan I [2 populations], 6850 [3], JE2

395 [1]), with *alsT* mutations occurring in a total of 22 clones. This suggests that mutations in *alsT*,
396 which encodes a glutamine transporter (Zeden et al. 2020), are generally advantageous in the
397 presence of PA supernatant. The lack of any other evidence for parallel evolution indicates
398 that SA populations of all strains adapted to PA supernatant in a highly diverse and individual
399 manner.
400

401 **Absence of strong associations between evolved genotypes and phenotypes confirms**
402 **highly diverse evolutionary trajectories in response to PA inhibitory molecules**

403 We used the mutational patters uncovered to construct evolutionary cladograms for each
404 population independently evolved in the presence of PA supernatant. Additionally, we mapped
405 three phenotypes (growth in PA supernatant + TSB, staphyloxanthin [STX] production,
406 hydrogen peroxide [H_2O_2] survival) onto the cladograms to identify links between genotypic
407 and phenotypic changes (Figure 9).

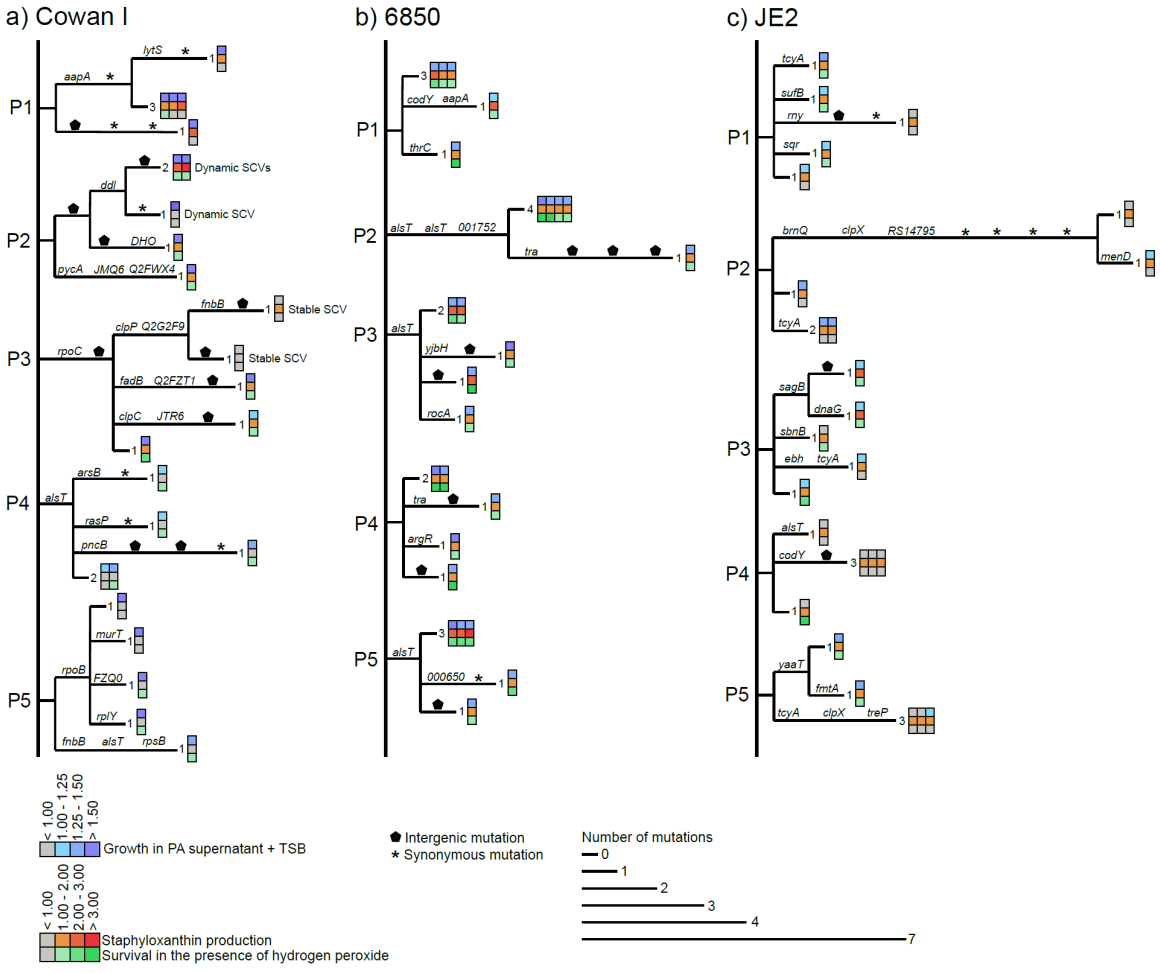

408

409 **Figure 9.** Cladograms showing within-population mutational patterns and their match to phenotypes of
410 SA clones evolved in the presence of PA supernatant. Separate cladograms are shown for each of the
411 five populations (P1 – P5) of the three SA strains (a) Cowan I, (b) 6850, and (c) JE2. Branch length
412 corresponds to the number of mutations per clone. Labels on branches indicate either nonsynonymous
413 mutations (gene name or abbreviated locus tag), intergenic mutations (pentagon), or synonymous
414 mutations (asterisk). Synonymous mutations were used to resolve branching patterns among clones.
415 Heatmaps on the tip of the branches show growth in the presence of PA supernatant (top row),
416 staphyloxanthin production (middle row), and survival in the presence of hydrogen peroxide (bottom
417 row) for the respective evolved clones, all expressed relative to the ancestor.
418

419 For Cowan I (Figure 9a), mutational patterns were highly diverse within and across
420 populations and there was no apparent link to any of the phenotypes. For example, while 23
421 out of 25 clones showed resistance to PA supernatant in terms of growth, the underlying
422 mutational patterns were extremely diverse.

423 For 6850 (Figure 9b), there is some evidence for parallel evolution via mutations in
424 *alsT*, which became fixed in three different populations. All clones with *alsT* mutations showed
425 higher growth, increased STX production and H_2O_2 survival. However, the same phenotypic
426 changes were also observed in other 6850 clones without *alsT* mutations. This shows that
427 mutations in different genes can lead to the same phenotypic changes.

428 For JE2 (Figure 9c), the genotype-phenotype matching was diverse, too. Overall, JE2
429 showed the least pronounced changes in phenotypes, most likely because the ancestor was
430 least affected by the PA supernatant (Figure 1). But when focusing on the clones in populations
431 P1, P3 and P5, which showed the most pronounced increases in growth, STX production and
432 H_2O_2, we found completely different underlying mutational patterns in each population. For
433 example, mutations in *tcyA* (population P1), *sagB* (P3), and *yaaT* (P5) all seemed to be
434 associated with the altered phenotypes. Only the *tcyA* gene, encoding a membrane
435 transporter, stood out from the other genes as it was repeatedly mutated in seven clones from
436 four different JE2 populations, suggesting that it plays a more general role in SA resistance
437 evolution.
438
439

440 **Discussion**

441 *Pseudomonas aeruginosa* (PA) and *Staphylococcus aureus* (SA) are among the most
442 important pathogens in polymicrobial infections, such as cystic fibrosis (CF) lung and wound
443 infections, and there is high interest in understanding how their interactions shape disease
444 outcome (Ibberson and Whiteley 2020; Limoli and Hoffman 2019). A large body of literature
445 has examined PA-SA interactions at the molecular level, and mostly described PA as the
446 dominant species suppressing the growth of SA by producing a variety of inhibitory molecules
447 (Hotterbeekx et al. 2017). However, because polymicrobial infections containing PA and SA
448 are often chronic, the two species may interact with each other (and with the host) over
449 prolonged periods of time, which could spur co-evolutionary dynamics, and the possibility of
450 SA to adapt to PA inhibitory molecules (Camus et al. 2021; Serra et al. 2015). Here, we tested
451 this hypothesis by exposing three different SA strains (Cowan I, 6850 and JE2) to the
452 supernatant, containing inhibitory molecules, of the PA reference strain PAO1, during
453 experimental evolution over 30 days. We found that all SA strains rapidly evolved resistance
454 to the growth inhibition imposed by PA. Using a combination of phenotypic and genotypic
455 assays, we show that (i) resistance evolution affected virulence traits, including increased
456 staphyloxanthin (STX) expression, higher survival in the presence of oxidative stress, small
457 colony variants (SCV) formation, and the maintenance of hemolysis; (ii) evolutionary
458 trajectories were highly SA strain-specific; and (iii) mutations in genes encoding membrane
459 transporters were the most frequent target of evolution. Our findings not only show that SA can
460 rapidly adapt to inhibitory molecules of PA, but also reveal that SA upregulates virulence traits
461 and modifies membrane transporters in response to PA supernatant exposure, evolutionary
462 changes that could lead to higher virulence and increased antibiotic resistance in infections.

463 All three SA strains were initially compromised in their growth by the PA supernatant,
464 and we confirmed that the *Pseudomonas* quinolone signal (PQS) molecule was directly
465 involved in growth inhibition. PQS does not only serve as a quorum-sensing signaling molecule
466 but also functions as an iron trap (Diggle et al. 2007). The iron-chelating activity of PQS
467 reduces the bioavailability of iron in the environment, and is known to inhibit a variety of gram-

468 negative and gram-positive bacterial species (Popat et al. 2017; Toyofuku et al. 2010). Here,
469 we show that it also has a strong inhibitory effect on SA. HQNO is another molecule produced
470 through the PQS synthesis cascade that has anti-SA properties via inhibition of the respiratory
471 chain (Hoffman et al. 2006). It is thus likely that the inhibitory effects on SA growth observed
472 in our supernatant assays is a combination of the effects of PQS and HQNO.

473 We found that the extent to which SA strains were inhibited and the strength of
474 resistance evolution towards the PA supernatant varied across SA strains (Figure 3). While
475 the Cowan I ancestor was greatly inhibited, it showed the largest improvement in growth after
476 evolution in the PA supernatant, and even outperformed the ancestral wildtype growing in TSB
477 alone. Similarly, 6850 was initially greatly inhibited by the PA supernatant, and all replicate
478 populations showed resistance evolution, reflected by a significantly improved growth. JE2
479 was initially the least inhibited strain, and while overall, we found significantly improved growth
480 after evolution, not all replicate populations followed this trend. It is perhaps unsurprising that
481 the most severely affected SA strains showed the strongest response in terms of resistance
482 evolution. However, it is interesting that the ancestral JE2 is the most virulent and most
483 competitive SA strain in our panel (Diep et al. 2006; Niggli and Kümmerli 2020). This suggests
484 that JE2 might already be well equipped to deal with PA inhibitory molecules, leaving less room
485 for further fitness improvements compared to the less virulent and less competitive Cowan I or
486 6850 strains.

487 During evolution, we observed that SA virulence traits were under selection and often
488 overproduced, which could have severe consequences in infections (Cheung, Bae, and Otto
489 2021; Pollitt et al. 2014). Importantly, the virulence traits under selection varied across SA
490 strains, reinforcing our notion that evolutionary responses to PA inhibitory molecules are SA
491 strain specific. Increased formation of SCVs evolved almost exclusively in Cowan I
492 populations. However, we assume that the true SCV frequency might be higher than the one
493 reported, because SCVs are difficult to detect. The formation of SA SCVs is a well-known
494 adaptive response towards stressful conditions (Kahl, Becker, and Löffler 2016), and we
495 propose that SCVs evolved in our experiment as a response to PA inhibitory molecules such

496 as HQNO (Hoffman et al. 2006). Due to their slow metabolism, SCVs frequently exhibit
497 reduced antibiotic susceptibility, which makes them particularly problematic in a clinical context
498 (Huemer et al. 2020). For 6850 clones, the strongest phenotypic changes involved increased
499 STX production and better survival in the presence of oxidative stress (H_2O_2 exposure).
500 Adaptations in 6850 therefore likely led to better protection against reactive oxygen species
501 (ROS) induced by PA inhibitory molecules, such as HQNO, pyocyanin, and PQS (Abdalla et
502 al. 2017; Noto et al. 2017; Tognon et al. 2019). In the context of infections, such adaptations
503 would be problematic, because innate host immune responses against pathogens typically
504 involve the production of ROS (Schieber and Chandel 2014). For JE2, we observed that
505 hemolysis was selectively maintained in the presence of PA supernatant but lost in its absence.
506 While hemolysis is an important virulence trait, it can be lost in chronic infections (Shopsin et
507 al. 2008; Traber et al. 2008). Our findings now suggest that the presence of PA could maintain
508 this trait and keep JE2 and related strains at a higher state of virulence.

509 At the genetic level, we found positive selection but little evidence for parallel evolution
510 across strains and populations upon exposure to the PA supernatant. This indicates that
511 mutations in many different genes were under selection and possibly contributed to resistance
512 evolution towards PA inhibitory molecules. The fact that mutations in a broad spectrum of
513 genes can promote resistance highlights the enormous evolvability of SA (Deurenberg and
514 Stobberingh 2008). In contrast, we found evidence for parallel evolution among clones that
515 evolved in the TSB medium alone, where we identified several genes (Table S2) that were
516 frequently mutated in independent populations and across strains. These findings show that,
517 whether or not parallel evolution occurs, depends on the environment and the specific selection
518 pressures that prevail therein.

519 Remarkable is that, although there was little evidence for parallel evolution at the gene
520 level in clones evolved in the presence of PA supernatant, we found parallelism at the
521 functional level, with many mutations occurring in membrane transport genes (Figure 8c). For
522 example, the gene encoding the glutamine transporter AlsT was mutated in 22 clones from six
523 populations across all three SA strains. While AlsT inactivation reduces the susceptibility of

524 SA to the toxic glutamine analogue γ-L-glutamyl hydrazide (Zeden et al. 2020), our results now
525 suggest that AlsT alterations might similarly reduce the uptake of PA inhibitory molecules.
526 Moreover, it was shown that loss-of-function mutations in *alsT* increase intracellular c-di-AMP
527 levels, which allows bacteria to better resist stressful conditions (Corrigan et al. 2011). Our
528 results support this notion and suggest that *alsT* mutations were selected for to withstand the
529 stress imposed by PA inhibitory molecules in the supernatant. Another example involves
530 mutations in the gene *tcyA*, which encodes a part of the cystine transporter TcyABC. While
531 mutations in this gene were unique to JE2, they surfaced in seven clones in four out of the five
532 JE2 populations. Deletion of *tcyA* leads to resistance against the toxic cystine analogue
533 selenocystine in SA (Lensmire et al. 2020). While PA strain PAO1 indeed contains the
534 selenocysteine synthesis cluster, it is currently not known how its expression is controlled and
535 whether selenocystine is deployed against competitors. Our data now suggest that it might
536 indeed play a role in competition, and that mutations in *tcyA* could be an evolutionary response
537 by SA to reduce selenocystine uptake. More generally, as membrane transport systems are
538 known to control virulence and antibiotic resistance in SA, they have been proposed as novel
539 targets for therapeutic agents (Zeden et al. 2021). Our finding that the exposure to PA inhibitory
540 molecules can select for SA variants with altered membrane transporters could therefore pose
541 a problem for drug design and therapy, as these mutants could be less susceptible to
542 antibiotics.

543 In summary, our work shows that SA rapidly and specifically adapts to PA inhibitory
544 molecules. Several virulence traits were upregulated or selectively maintained in response to
545 PA supernatant exposure, and our genomic analysis revealed that mutations in membrane
546 transport genes are associated with resistance evolution in SA. Such adaptations could have
547 severe implications for infections, as SA virulence might be increased, and baseline levels of
548 antibiotic resistance might arise even before a treatment is applied. A key next step would
549 involve testing whether the observed increases in virulence trait expression and mutations in
550 membrane transporters lead to altered virulence and antibiotic susceptibility profiles *in vivo*.
551 Moreover, while we focused on SA evolution and others on PA evolution (Tognon et al. 2017),

552 we next need to study co-evolution to understand the patterns and consequences of reciprocal
553 adaptation in both species, as they might occur in polymicrobial infections (Rezzoagli, Granato,
554 and Kümmerli 2020). In a broader context, the fact that evolutionary trajectories were strongly
555 SA strain-specific, suggests that we ultimately need to understand polymicrobial dynamics and
556 its consequences at an 'individualized' patient-by-patient level to identify optimal personalized
557 treatment strategies for each case.
558

559 **Materials and Methods**

560 **Bacterial strains, media, and growth conditions**

561 We used *Pseudomonas aeruginosa* (PA) strain PAO1 (ATCC 15692) and the three genetically
562 different *Staphylococcus aureus* (SA) strains Cowan I, 6850 and JE2 (Table S1) for all our
563 experiments. All growth experiments and the experimental evolution were performed in tryptic
564 soy broth (TSB, Becton Dickinson, Heidelberg, Germany) medium. Overnight cultures (prior to
565 experimental evolution) were grown in 10 ml TSB in 50 ml falcon tubes at 37 °C and 220 rpm
566 with aeration. The phenotypic assays after experimental evolution involved large sample sizes
567 including many evolved clones, populations, and the respective ancestors. For this reason, we
568 grew overnights in 24-well plates filled with 1.5 ml TSB per well at 37 °C and 170 rpm.
569

570 **Supernatant assays**

571 To test whether the supernatant of PA inhibits SA (and vice versa) we performed supernatant
572 growth assays as follows. We first generated cell-free supernatants by growing PA and SA
573 donor strains overnight in TSB. After centrifugation of the cultures to pellet cells, we sterile-
574 filtered the supernatant using 0.2 µm pore size filters (Whatman, Fisher Scientific, Reinach,
575 Switzerland) and stored aliquots of the supernatant at -20 °C. For the supernatant assay, we
576 grew PA and SA receiver strains overnight, washed bacterial cell pellets with 10 ml 0.8% NaCl
577 and adjusted OD_{600} (optical density at 600 nm) to obtain comparable cell numbers per ml for
578 all strains. To achieve this, we adjusted OD_{600} of PA to 1.0, for SA strains JE2 and 6850 to 0.4
579 and for Cowan I to 0.8. Subsequently, we diluted the PA inoculum 1:100,000 and the SA

580 inoculums 1:10,000 to start our experiments. PA was diluted more because it grows faster
581 compared to SA. The diluted inoculums were prepared in the following three media conditions:
582 (1) 100% TSB (as growth control); (2) 30% NaCl solution + 70% TSB (control to mimic reduced
583 nutrient availability); (3) 30% PA or SA supernatant + 70% TSB (condition of interest).
584 Supernatant assays were performed in 96-well plates with 200 µl per well. We
585 incubated plates statically at 37 °C in a plate reader (Tecan Infinite M nano, Tecan, Männedorf,
586 Switzerland) and measured growth of strains by recording OD_{600} every 30 min for 48 hours,
587 with 30 sec shaking events prior to recordings. Effect of PA supernatant on growth of SA strains
588 was assessed in seven independent experiments and effect of SA supernatants on PA growth
589 was assessed in one experiment per SA supernatant. In every assay, we used four replicates
590 per strain and growth condition.
591
592 **SA growth in the presence of PQS**
593 To test whether PQS (heptyl-3-hydroxy-4(1H)-quinolone, Sigma-Aldrich, Buchs, Switzerland)
594 is involved in the growth inhibition of SA, we exposed cultures of all three SA strains to final
595 concentrations of 20 µM, 50 µM or 80 µM PQS (10 mM stock in DMSO), supplemented to the
596 TSB growth medium, and compared their growth relative to the growth in TSB supplemented
597 with DMSO alone (same volume of DMSO as for the 80 µM PQS treatment). SA strain
598 preparation and growth measurements followed the same protocol as for the supernatant
599 assays.
600
601 **Experimental evolution of SA in the presence or absence of PA supernatant**
602 To elucidate whether and how SA strains respond to the presence of PA supernatant over
603 time, we performed an experimental evolution experiment, in which we exposed the three SA
604 strains Cowan I, 6850 and JE2 for 30 days to either 30% PA supernatant + 70% TSB
605 (experimental treatment) or 100% TSB (control treatment). Experimental evolution started from
606 clonal populations. We had seven independent populations per strain and condition, resulting
607 in a total of 42 evolving populations, distributed on 96-well plates (one plate per SA ancestor).

608 All populations were incubated statically at 37 °C. Every 48 hours, we diluted and transferred
609 the evolving cultures 1:10,000 into fresh medium and recorded OD_{600} as a proxy for growth
610 prior to each transfer using a plate reader (Tecan Infinite M nano). To the part of the culture
611 that was not transferred, we added equal volumes of a sterile 85% glycerol solution directly
612 into the wells of the 96-well plate and froze them at -80 °C as a backup. Overall, the experiment
613 ran for 30 days (15 transfers). Based on a pre-experiment, we estimated the mean number of
614 doublings (± standard deviation) for the three SA ancestors in the two growth conditions during
615 a 48-hour growth cycle as follows: for Cowan I: 14.5 ± 0.4 (in TSB) / 9.2 ± 0.7 (in PA
616 supernatant + TSB); for 6850: 14.3 ± 0.8 / 10.6 ± 1.7; for JE2: 14.6 ± 0.5 / 13.5 ± 0.6. Thus,
617 our experimental evolution involved at least 140 - 220 bacterial generations (assuming no
618 evolutionary improvements in growth). Following experimental evolution, we plated all evolved
619 populations on 1.2% TSB agar and randomly picked five clones per population for further
620 characterization. All selected clones were first cultured overnight in TSB and then frozen at -
621 80 °C by mixing 50% of culture with 50% of a sterile 85% glycerol solution.
622
623 **Growth of evolved populations and clones**
624 We tested whether the 42 evolved populations and the selected 210 clones showed improved
625 growth performance relative to the ancestors in the two conditions of our experimental
626 evolution (30% PA supernatant + 70% TSB and 100% TSB). We exposed all populations and
627 clones to the condition they had evolved in, but also to the alternate condition they had not
628 evolved in. For this growth screening, we followed the exact same protocol as the one
629 described above for the supernatant assay.
630
631 **Staphyloxanthin (STX) quantification**
632 For the subsequent phenotypic and genotypic assays, we used a total of 150 clones from 30
633 populations (5 clones per population). Sample size was reduced to meet the sequencing
634 contingent of this project. In a first assay, we tested whether evolved clones changed
635 staphyloxanthin (STX) production compared to the respective ancestor. We quantified this SA

636 pigment based on a previously published protocol (Antonic et al. 2013). Briefly, we first
637 collected 1 ml from each culture of all evolved clones and ancestors (grown overnight in TSB)
638 and resuspended washed pellets in 400 µl methanol. We incubated the samples for 10 min at
639 55 °C, pelleted cells by centrifugation and collected the supernatant containing the STX.
640 Absorbance of the crude extract was measured in duplicates at λ = 465 nm using a plate reader
641 (Tecan Infinite M200 pro). We blank-corrected STX values and expressed them first, relative
642 to the blank-corrected OD_{600} of the respective clone and second, relative to the respective STX
643 value of the ancestor.
644
645 **Hydrogen peroxide (H_2O_2) survival assay**
646 To determine whether evolved clones are better at surviving under oxidative stress conditions,
647 we performed a hydrogen peroxide (H_2O_2) survival assay, which we adapted from a previously
648 published protocol (Hall et al. 2017). In short, we subjected cultures of all evolved clones and
649 ancestors (grown overnight in TSB) to either 1.5% H_2O_2 or 0.8% NaCl (as control) for one hour
650 at 37 °C. Subsequently, we plated dilutions on 1.2% TSB agar, incubated plates overnight at
651 37 °C and enumerated colony forming units (CFUs) on the next day. We then calculated the
652 percentage survival for each clone as the CFUs from the H_2O_2 treatment divided by the CFUs
653 from the control treatment multiplied by 100.
654
655 **Small colony variant (SCV) detection and quantification**
656 To determine whether evolved clones express SCV phenotypes, we plated cultures of all
657 evolved clones on 1.2% TSB agar, incubated plates overnight at 37 °C, and then classified the
658 colonies with an area smaller than 20% of the ancestral colony size as SCV. To estimate the
659 prevalence of SCVs at the population level, we also serially diluted and plated aliquots of every
660 evolved population on 1.2% TSB agar and assessed the percentage of SCVs per population
661 after incubation of plates overnight at 37 °C.
662
663

664 **Hemolysis assay**

665 The ancestral strains of 6850 and JE2 are known for their ability to lyse red blood cells
666 (hemolysis), whereas Cowan I is unable to do so. To determine whether evolved clones of
667 6850 and JE2 show different hemolysis patterns compared to their ancestors, we plated
668 cultures of all evolved clones and ancestors (grown overnight in TSB) on COS plates (columbia
669 agar + 5% sheep blood, Biomérieux, Petit-Lancy, Switzerland). COS plates were incubated
670 overnight at 37 °C. On the next day, we qualitatively assessed the hemolysis pattern of each
671 clone according to three discrete categories: ancestral-like hemolysis (wild-type like), reduced
672 hemolysis, (almost) absent hemolysis (examples depicted in Figure 6c). In addition, we also
673 plated all evolved populations on COS plates to assess the frequency of the three hemolysis
674 phenotypes within populations.

675

676 **Genome sequencing**

677 To identify genetic changes in evolved clones relative to their ancestors, we extracted the
678 genomic DNA of all 150 phenotypically characterized clones and the three ancestral SA
679 strains. We used the Maxwell RSC Cultured Cells DNA Kit (Promega, Dübendorf, Switzerland)
680 together with the Maxwell RSC 48 instrument (Promega) following the manufacturer's protocol.
681 To lyse the gram-positive SA cells, we added lysostaphin (L7386, Sigma-Aldrich) to the
682 samples (final concentration of 25 µg per 400 µl sample). DNA concentrations were quantified
683 using the QuantiFluor dsDNA sample kit (Promega). Library preparation was performed with
684 100 ng of DNA input using the TruSeq DNA Nano kit (Illumina, San Diego, USA) according to
685 the manufacturers' instructions. The libraries were quantified using the Tapestation (Agilent
686 Technologies, Santa Clara, USA) and qPCR (Roche, Rotkreuz, Switzerland) and equimolarly
687 pooled. Finally, the libraries were sequenced 150 bp paired-end on the NovaSeq6000 system
688 (Illumina, San Diego, USA). The samples had an estimated coverage of 100x for the evolved
689 clones and 200x for the three SA ancestors.

690 The quality of the raw sequencing data was assessed using FastQC (version 0.11.9)
691 (https://www.bioinformatics.babraham.ac.uk/projects/fastqc/) and a contamination check was

692 performed using Fastqscreen (version 0.14.1). Subsequently, the raw reads were
693 preprocessed using Trimmomatic (Bolger, Lohse, and Usadel 2014) with the following settings:
694 trimmString="ILLUMINACLIP: adapters.fa:1:30:10 LEADING:15 TRAILING:15
695 SLIDINGWINDOW:5:30 AVGQUAL:32 MINLEN:80". All the reads that passed the trimming
696 and quality filtering steps were analyzed using Snippy (https://github.com/tseemann/snippy)
697 (v4.5.2) with default parameters. For the ancestral strains 6850 and JE2, the reads were
698 aligned to the published reference genomes (GenBank accession Nr. CP006706.1 and
699 NZ_CP020619.1, respectively). Variants that were present in the ancestor compared to the
700 published reference genome were removed and only those variants that occurred during
701 experimental evolution were kept. Finally, we used SnpEff version 4.3t (built 2017-11-24 10:18)
702 (https://pcingola.github.io/SnpEff/) to predict variant effects. For Cowan I, no suitable reference
703 genome was available, and we thus performed a *de novo* assembly with SPAdes (v3.12.0)
704 and annotation with Prodigal (v2.6.3) using the reads from our ancestor, and then directly
705 called the variants as in the other two strains for the evolved clones relative to the *de novo*
706 assembled ancestral genome. Note that one clone had to be discarded after library preparation
707 due to poor DNA quality.
708
709 **Statistical analysis**
710 All statistical analyses were performed with R Studio version 3.6.3. We used general linear
711 models wherever possible and consulted Q-Q plots and the Shapiro-Wilk test to examine
712 whether residuals were normally distributed. The basic linear model that we used was an
713 analysis of variance (ANOVA) in which we put the response variable in relation to the
714 manipulated factors, which are (i) the SA strain background (Cowan I, 6850, JE2), (ii) the
715 experimental conditions (presence/absence of PA supernatant or PQS concentration), and (iii)
716 the interaction between the two. We used variants of this model for statistical analysis of all
717 growth data, STX production, and survival in the presence of H_2O_2 as response variables. Non-
718 significant interactions were removed from the models. If data was not normally distributed (as

719 for the survival data), we $\log_{10}(x+1)$-transformed all values for statistical analysis and scaled
720 them back to the respective ancestor for plotting.

721 We performed one sample t-tests to test whether STX production and survival in the
722 presence of H_2O_2 in evolved clones was significantly different from the expected ancestral
723 value. The false discovery rate method was used to correct p-values whenever necessary. For
724 frequency comparisons between hemolysis categories for 6850 and JE2 clones evolved in the
725 two media, we performed Fisher's exact tests. The principle component analysis (PCA) was
726 performed on clonal phenotypes using the *vegan* package in R. We tested for inference using
727 permutational multivariate analysis of variance (PERMANOVA).

728 **Competing interests**

729 The authors declare that no competing interests exist.

730

731 **Author Contributions**

732 S.N. and R.K. designed research, S.N. performed research, L.P. and J.G. analyzed the
733 genome sequencing data, S.N. and R.K. analyzed all other datasets and wrote the paper with
734 inputs from L.P. and J.G. All authors approved the manuscript prior to submission.

735

736 **Funding**

737 This project has received funding from the European Research Council under the European
738 Union's Horizon 2020 research and innovation program (grant agreement no. 681295) to RK,
739 from the Swiss National Science Foundation (31003A_182499) to RK, and from the University
740 of Zürich Teaching Fund (2019_12 / Fostering OMICS research through research- based
741 teaching and learning) to LP and JG.

742

743 **Acknowledgements**

744 We thank Markus Huemer and Annelies Zinkernagel (University Hospital of Zürich) for
745 providing *S. aureus* strains, the Eberl group (University of Zürich) for providing the *P.*
746 *aeruginosa ΔpqsA* strain, Jay Tracy for helping with DNA extraction, Maria Domenica Moccia
747 for performing the whole genome sequencing, Giancarlo Russo for bioinformatic analysis, and
748 Alexandre Figueiredo for comments about the manuscript. Illustration for Supplementary
749 Figure 4 was created using BioRender (www.biorender.com).

750

751 **Data availability statement**

752 All raw data sets will be deposited in an online repository upon the acceptance of the
753 manuscript.

754

755 **References**

756 Abdalla, Maher Y., Traci Hoke, Javier Seravalli, Barbara L. Switzer, Melissa Bavitz, Jill D.
757 Fliege, Peter J. Murphy, and Bradley E. Britigan. 2017. "Pseudomonas Quinolone
758 Signal Induces Oxidative Stress and Inhibits Heme Oxygenase-1 Expression in Lung
759 Epithelial Cells." *Infection and Immunity* 85 (9): 1–14. https://doi.org/doi:
760 10.1128/IAI.00176-17.

761 Antonic, Vlado, Alexander Stojadinovic, Binxue Zhang, Mina J. Izadjoo, and Mohammad
762 Alavi. 2013. "Pseudomonas Aeruginosa Induces Pigment Production and Enhances
763 Virulence in a White Phenotypic Variant of Staphylococcus Aureus." *Infection and Drug*
764 *Resistance* 6: 175–86. https://doi.org/10.2147/IDR.S49039.

765 Biswas, Lalitha, Raja Biswas, Martin Schlag, Ralph Bertram, and Friedrich Götz. 2009.
766 "Small-Colony Variant Selection as a Survival Strategy for Staphylococcus Aureus in the
767 Presence of Pseudomonas Aeruginosa." *Applied and Environmental Microbiology* 75
768 (21): 6910–12. https://doi.org/10.1128/AEM.01211-09.

769 Bolger, Anthony M., Marc Lohse, and Bjoern Usadel. 2014. "Trimmomatic: A Flexible
770 Trimmer for Illumina Sequence Data." *Bioinformatics* 30 (15): 2114–20.
771 https://doi.org/10.1093/bioinformatics/btu170.

772 Bredenbruch, Florian, Robert Geffers, Manfred Nimtz, Jan Buer, and Susanne Häussler.
773 2006. "The Pseudomonas Aeruginosa Quinolone Signal (PQS) Has an Iron-Chelating
774 Activity." *Environmental Microbiology* 8 (8): 1318–29. https://doi.org/10.1111/j.1462-
775 2920.2006.01025.x.

776 Brogden, Kim A, Janet M Guthmiller, and Christopher E Taylor. 2005. "Human Polymicrobial
777 Infections." *Lancet* 365 (9455): 253–55. https://doi.org/https://doi.org/10.1016/S0140-
778 6736(05)17745-9.

779 Burnside, Kellie, Annalisa Lembo, Melissa de los Reyes, Anton Iliuk, Nguyen Thao BinhTran,
780 James E. Connelly, Wan Jung Lin, et al. 2010. "Regulation of Hemolysin Expression
781 and Virulence of Staphylococcus Aureus by a Serine/Threonine Kinase and
782 Phosphatase." *PLoS ONE* 5 (6). https://doi.org/10.1371/journal.pone.0011071.

783 Camus, Laura, Paul Briaud, François Vandenesch, and Karen Moreau. 2021. “How Bacterial
784 Adaptation to Cystic Fibrosis Environment Shapes Interactions Between Pseudomonas
785 Aeruginosa and Staphylococcus Aureus.” *Frontiers in Microbiology* 12 (March): 1–16.
786 https://doi.org/10.3389/fmicb.2021.617784.
787 Cheung, Gordon Y.C., Justin S. Bae, and Michael Otto. 2021. “Pathogenicity and Virulence
788 of Staphylococcus Aureus.” *Virulence* 12 (1): 547–69.
789 https://doi.org/10.1080/21505594.2021.1878688.
790 Clauditz, Alexandra, Alexandra Resch, Karsten Peter Wieland, Andreas Peschel, and
791 Friedrich Götz. 2006. “Staphyloxanthin Plays a Role in the Fitness of Staphylococcus
792 Aureus and Its Ability to Cope with Oxidative Stress.” *Infection and Immunity* 74 (8):
793 4950–53. https://doi.org/10.1128/IAI.00204-06.
794 Corrigan, Rebecca M., James C. Abbott, Heike Burhenne, Volkhard Kaever, and Angelika
795 Gründling. 2011. “C-Di-AMP Is a New Second Messenger in Staphylococcus Aureus
796 with a Role in Controlling Cell Size and Envelope Stress.” *PLoS Pathogens* 7 (9).
797 https://doi.org/10.1371/journal.ppat.1002217.
798 Dalton, Trevor, Scot E. Dowd, Randall D. Wolcott, Yan Sun, Chase Watters, John A.
799 Griswold, and Kendra P. Rumbaugh. 2011. “An in Vivo Polymicrobial Biofilm Wound
800 Infection Model to Study Interspecies Interactions.” *PLoS ONE* 6 (11).
801 https://doi.org/10.1371/journal.pone.0027317.
802 Deurenberg, Ruud H., and Ellen E. Stobberingh. 2008. “The Evolution of Staphylococcus
803 Aureus.” *Infection, Genetics and Evolution* 8 (6): 747–63.
804 https://doi.org/10.1016/j.meegid.2008.07.007.
805 Diep, Binh An, Steven R. Gill, Richard F. Chang, Tiffany HaiVan Phan, Jason H. Chen,
806 Matthew G. Davidson, Felice Lin, et al. 2006. “Complete Genome Sequence of
807 USA300, an Epidemic Clone of Community-Acquired Meticillin-Resistant
808 Staphylococcus Aureus.” *Lancet* 367 (4): 731–39. https://doi.org/DOI: 10.1016/S0140-
809 6736(06)68231-7.
810 Diggle, Stephen P., Sandra Matthijs, Victoria J. Wright, Matthew P. Fletcher, Siri Ram

811 Chhabra, Iain L. Lamont, Xiaole Kong, et al. 2007. “The Pseudomonas Aeruginosa 4-
812 Quinolone Signal Molecules HHQ and PQS Play Multifunctional Roles in Quorum
813 Sensing and Iron Entrapment.” *Chemistry and Biology* 14 (1): 87–96.
814 https://doi.org/10.1016/j.chembiol.2006.11.014.
815 Dowd, Scot E., Yan Sun, Patrick R. Secor, Daniel D. Rhoads, Benjamin M. Wolcott, Garth A.
816 James, and Randall D. Wolcott. 2008. “Survey of Bacterial Diversity in Chronic Wounds
817 Using Pyrosequencing, DGGE, and Full Ribosome Shotgun Sequencing.” *BMC*
818 *Microbiology* 8 (43): 1–15. https://doi.org/10.1186/1471-2180-8-43.
819 Dubern, Jean Frédéric, and Stephen P. Diggle. 2008. “Quorum Sensing by 2-Alkyl-4-
820 Quinolones in Pseudomonas Aeruginosa and Other Bacterial Species.” *Molecular*
821 *BioSystems* 4 (9): 882–88. https://doi.org/10.1039/b803796p.
822 Fazli, Mustafa, Thomas Bjarnsholt, Klaus Kirketerp-Møller, Bo Jørgensen, Anders Schou
823 Andersen, Karen A. Krogfelt, Michael Givskov, and Tim Tolker-Nielsen. 2009.
824 “Nonrandom Distribution of Pseudomonas Aeruginosa and Staphylococcus Aureus in
825 Chronic Wounds.” *Journal of Clinical Microbiology* 47 (12): 4084–89.
826 https://doi.org/10.1128/JCM.01395-09.
827 Filkins, Laura M., Jyoti A. Graber, Daniel G. Olson, Emily L. Dolben, Lee R. Lynd, Sabin
828 Bhuju, and George A. O’Toole. 2015. “Coculture of Staphylococcus Aureus with
829 Pseudomonas Aeruginosa Drives S. Aureus towards Fermentative Metabolism and
830 Reduced Viability in a Cystic Fibrosis Model.” *Journal of Bacteriology* 197 (14): 2252–
831 64. https://doi.org/10.1128/JB.00059-15.
832 Fuchs, Stephan, Henry Mehlan, Jörg Bernhardt, André Hennig, Stephan Michalik, Kristin
833 Surmann, Jan Pané-Farré, et al. 2018. “AureoWiki‐The Repository of the
834 Staphylococcus Aureus Research and Annotation Community.” *International Journal of*
835 *Medical Microbiology* 308 (6): 558–68. https://doi.org/10.1016/j.ijmm.2017.11.011.
836 Gangell, Catherine, Samantha Gard, Tonia Douglas, Judy Park, Nicholas De Klerk, Tony
837 Keil, Siobhain Brennan, Sarath Ranganathan, Roy Robins-Browne, and Peter D. Sly.
838 2011. “Inflammatory Responses to Individual Microorganisms in the Lungs of Children

with Cystic Fibrosis." *Clinical Infectious Diseases* 53 (5): 425–32. https://doi.org/10.1093/cid/cir399.

Gjødsbøl, Kristine, Jens Jørgen Christensen, Tonny Karlsmark, Bo Jørgensen, Bjarke M. Klein, and Karen A. Krogfelt. 2006. "Multiple Bacterial Species Reside in Chronic Wounds: A Longitudinal Study." *International Wound Journal* 3 (3). https://doi.org/10.1111/j.1742-481X.2006.00159.x.

Hall, Jeffrey W, Junshu Yang, Haiyong Guo, and Yinduo Ji. 2017. "The Staphylococcus Aureus AirSR Two- Component System Mediates Reactive Oxygen Species Resistance via Transcriptional Regulation of Staphyloxanthin Production." *Infection and Immunity* 85 (2): 1–12. https://doi.org/DOI: 10.1128/IAI.00838-16.

Harrison, Freya, Jon Paul, Ruth C. Massey, and Angus Buckling. 2008. "Interspecific Competition and Siderophore-Mediated Cooperation in Pseudomonas Aeruginosa." *ISME Journal* 2 (1): 49–55. https://doi.org/10.1038/ismej.2007.96.

Hendricks, Kelly J., Tim A. Burd, Jeffrey O. Anglen, Andrew W. Simpson, Gordon D. Christensen, and Barry J. Gainor. 2001. "Synergy Between Staphylococcus Aureus and Pseudomonas Aeruginosa in a Rat Model of Complex Orthopaedic Wounds." *The Journal of Bone & Joint Surgery* 83 (6). https://doi.org/DOI:10.2106/00004623-200106000-00006.

Hoffman, Lucas R., Eric Déziel, David A. D'Argenio, François Lépine, Julia Emerson, Sharon McNamara, Ronald L. Gibson, Bonnie W. Ramsey, and Samuel I. Miller. 2006. "Selection for Staphylococcus Aureus Small-Colony Variants Due to Growth in the Presence of Pseudomonas Aeruginosa." *Proceedings of the National Academy of Sciences of the United States of America* 103 (52): 19890–95. https://doi.org/10.1073/pnas.0606756104.

Hotterbeekx, An, Samir Kumar-Singh, Herman Goossens, and Surbhi Malhotra-Kumar. 2017. "In Vivo and In Vitro Interactions between Pseudomonas Aeruginosa and Staphylococcus Spp." *Frontiers in Cellular and Infection Microbiology* 7 (APR): 1–13. https://doi.org/10.3389/fcimb.2017.00106.

867 Hubert, Dominique, Hélène Réglier-Poupet, Isabelle Sermet-Gaudelus, Agnès Ferroni,
868 Muriel Le Bourgeois, Pierre Régis Burgel, Raphaël Serreau, Daniel Dusser, Claire
869 Poyart, and Joël Coste. 2013. "Association between Staphylococcus Aureus Alone or
870 Combined with Pseudomonas Aeruginosa and the Clinical Condition of Patients with
871 Cystic Fibrosis." *Journal of Cystic Fibrosis* 12 (5): 497–503.
872 https://doi.org/10.1016/j.jcf.2012.12.003.
873 Huemer, Markus, Srikanth Mairpady Shambat, Silvio D Brugger, and Annelies S Zinkernagel.
874 2020. "Antibiotic Resistance and Persistence—Implications for Human Health and
875 Treatment Perspectives." *EMBO Reports* 21 (12): 1–24.
876 https://doi.org/10.15252/embr.202051034.
877 Ibberson, Carolyn B., and Marvin Whiteley. 2020. "The Social Life of Microbes in Chronic
878 Infection." *Current Opinion in Microbiology* 53: 44–50.
879 https://doi.org/10.1016/j.mib.2020.02.003.
880 Jorge, Luciana Souza, Patrícia Silva Fucuta, Maria Gabriele L., Marcelo Arruda Nakazone,
881 Juliana Arruda de, Alceu Gomes Chueire, and Mauro José Costa. 2018. "Outcomes and
882 Risk Factors for Polymicrobial Posttraumatic Osteomyelitis." *Journal of Bone and Joint*
883 *Infection* 3 (1): 20–26. https://doi.org/10.7150/jbji.22566.
884 Kahl, Barbara C, Karsten Becker, and Bettina Löffler. 2016. "Clinical Significance and
885 Pathogenesis of Staphylococcal Small Colony Variants in Persistent Infections."
886 *American Society for Microbiology* 29 (2): 401–27. https://doi.org/10.1128/CMR.00069-
887 15.
888 Kessler, E., M. Safrin, J. C. Olson, and D. E. Ohman. 1993. "Secreted LasA of Pseudomonas
889 Aeruginosa Is a Staphylolytic Protease." *Journal of Biological Chemistry* 268 (10):
890 7503–8.
891 Leimer, Nadja, Carole Rachmühl, Miguel Palheiros Marques, Anna Sophie Bahlmann,
892 Alexandra Furrer, Fritz Eichenseher, Kati Seidl, et al. 2016. "Nonstable Staphylococcus
893 Aureus Small-Colony Variants Are Induced by Low PH and Sensitized to Antimicrobial
894 Therapy by Phagolysosomal Alkalinization." *Journal of Infectious Diseases* 213 (2):

895 305–13. https://doi.org/10.1093/infdis/jiv388.
896 Lensmire, Joshua M, Jack P Dodson, Brian Y Hsueh, Michael R Wischer, Phillip C Delekta,
897 John C Shook, Elizabeth N Ottosen, Paige J Kies, Janani Ravi, and Neal D. Hammer.
898 2020. “The Staphylococcus Aureus Cystine Transporters TcyABC and TcyP Facilitate
899 Nutrient Sulfur Acquisition during Infection.” *Infection and Immunity* 88 (3).
900 https://doi.org/https://doi.org/10.1128/IAI.00690-19.
901 Lim, Nigel C.S., Dawn K.A. Lim, and Manotosh Ray. 2013. “Polymicrobial versus
902 Monomicrobial Keratitis: A Retrospective Comparative Study.” *Eye and Contact Lens* 39
903 (5): 348–54. https://doi.org/10.1097/ICL.0b013e3182a3024e.
904 Limoli, Dominique H., and Lucas R. Hoffman. 2019. “Help, Hinder, Hide and Harm: What
905 Can We Learn from the Interactions between Pseudomonas Aeruginosa and
906 Staphylococcus Aureus during Respiratory Infections.” *Thorax* 74 (7): 684–92.
907 https://doi.org/10.1136/thoraxjnl-2018-212616.
908 Lin, Jinshui, Juanli Cheng, Yao Wang, and Xihui Shen. 2018. “The Pseudomonas Quinolone
909 Signal (PQS): Not Just for Quorum Sensing Anymore.” *Frontiers in Cellular and*
910 *Infection Microbiology* 8 (JUL): 1–9. https://doi.org/10.3389/fcimb.2018.00230.
911 Maliniak, Maret L., Arlene A. Stecenko, and Nael A. McCarty. 2016. “A Longitudinal Analysis
912 of Chronic MRSA and Pseudomonas Aeruginosa Co-Infection in Cystic Fibrosis: A
913 Single-Center Study.” *Journal of Cystic Fibrosis* 15 (3): 350–56.
914 https://doi.org/10.1016/j.jcf.2015.10.014.
915 Mashburn, Lauren M., Amy M. Jett, Darrin R. Akins, and Marvin Whiteley. 2005.
916 “Staphylococcus Aureus Serves as an Iron Source for Pseudomonas Aeruginosa during
917 in Vivo Coculture.” *Journal of Bacteriology* 187 (2): 554–66.
918 https://doi.org/10.1128/JB.187.2.554-566.2005.
919 Nguyen, Angela T., and Amanda G. Oglesby-Sherrouse. 2016. “Interactions between
920 Pseudomonas Aeruginosa and Staphylococcus Aureus during Co-Cultivations and
921 Polymicrobial Infections.” *Applied Microbiology and Biotechnology* 100 (14): 6141–48.
922 https://doi.org/10.1007/s00253-016-7596-3.

923 Niggli, Selina, and Rolf Kümmerli. 2020. “Strain Background, Species Frequency, and
924 Environmental Conditions Are Important in Determining Pseudomonas Aeruginosa and
925 Staphylococcus Aureus Population Dynamics and Species Coexistence.” *Applied and*
926 *Environmental Microbiology* 86 (18): 1–14. https://doi.org/DOI: 10.1128/AEM.00962-20.
927 Noto, Michael J., William J. Burns, William N. Beavers, and Eric P. Skaar. 2017.
928 “Mechanisms of Pyocyanin Toxicity and Genetic Determinants of Resistance in
929 Staphylococcus Aureus.” *Journal of Bacteriology* 199 (17): 1–13.
930 https://doi.org/10.1128/JB.00221-17.
931 Orazi, Giulia, and George A. O’Toole. 2017. “Pseudomonas Aeruginosa Alters
932 Staphylococcus Aureus Sensitivity to Vancomycin in a Biofilm Model of Cystic Fibrosis
933 Infection.” *MBio* 8 (4): 1–17. https://doi.org/10.1128/mBio.00873-17.
934 Pammi, Mohan, Danni Zhong, Yvette Johnson, Paula Revell, and James Versalovic. 2014.
935 “Polymicrobial Bloodstream Infections in the Neonatal Intensive Care Unit Are
936 Associated with Increased Mortality: A Case-Control Study.” *BMC Infectious Diseases*
937 14 (1): 1–8. https://doi.org/10.1186/1471-2334-14-390.
938 Pastar, Irena, Aron G. Nusbaum, Joel Gil, Shailee B. Patel, Juan Chen, Jose Valdes, Olivera
939 Stojadinovic, Lisa R. Plano, Marjana Tomic-Canic, and Stephen C. Davis. 2013.
940 “Interactions of Methicillin Resistant Staphylococcus Aureus USA300 and
941 Pseudomonas Aeruginosa in Polymicrobial Wound Infection.” *PLoS ONE* 8 (2): 1–11.
942 https://doi.org/10.1371/journal.pone.0056846.
943 Peters, Brian M., Mary Ann Jabra-Rizk, Graeme A. O’May, J. William Costerton, and Mark E.
944 Shirtliff. 2012. “Polymicrobial Interactions: Impact on Pathogenesis and Human
945 Disease.” *Clinical Microbiology Reviews* 25 (1): 193–213.
946 https://doi.org/10.1128/CMR.00013-11.
947 Phalak, Poonam, Jin Chen, Ross P. Carlson, and Michael A. Henson. 2016. “Metabolic
948 Modeling of a Chronic Wound Biofilm Consortium Predicts Spatial Partitioning of
949 Bacterial Species.” *BMC Systems Biology* 10 (1): 1–20. https://doi.org/10.1186/s12918-
950 016-0334-8.

951 Pollitt, Eric J.G., Stuart A. West, Shanika A. Crusz, Maxwell N. Burton-Chellew, and Stephen
952 P. Diggle. 2014. “Cooperation, Quorum Sensing, and Evolution of Virulence in
953 Staphylococcus Aureus.” *Infection and Immunity* 82 (3): 1045–51.
954 https://doi.org/10.1128/IAI.01216-13.
955 Popat, Roman, Freya Harrison, Ana C. da Silva, Scott A.S. Easton, Luke McNally, Paul
956 Williams, and Stephen P. Diggle. 2017. “Environmental Modification via a Quorum
957 Sensing Molecule Influences the Social Landscape of Siderophore Production.”
958 *Proceedings of the Royal Society B: Biological Sciences* 284 (1852).
959 https://doi.org/10.1098/rspb.2017.0200.
960 Ramos, Ana F., David F. Woods, Rachel Shanahan, Rafael Cano, Gerard P. McGlacken,
961 Claudia Serra, Fergal O’Gara, and F. Jerry Reen. 2020. “A Structure-Function Analysis
962 of Interspecies Antagonism by the 2-Heptyl-4-Alkyl-Quinolone Signal Molecule from
963 Pseudomonas Aeruginosa.” *Microbiology* 166 (2): 169–79.
964 https://doi.org/10.1099/mic.0.000876.
965 Rezzoagli, Chiara, Elisa T. Granato, and Rolf Kümmerli. 2020. “Harnessing Bacterial
966 Interactions to Manage Infections: A Review on the Opportunistic Pathogen
967 Pseudomonas Aeruginosa as a Case Example.” *Journal of Medical Microbiology* 69 (2):
968 147–61. https://doi.org/10.1099/jmm.0.001134.
969 Schieber, Michael, and Navdeep S. Chandel. 2014. “ROS Function in Redox Signaling and
970 Oxidative Stress.” *Current Biology* 24 (10): R453–62.
971 https://doi.org/10.1016/j.cub.2014.03.034.
972 Serra, Raffaele, Raffaele Grande, Lucia Butrico, Alessio Rossi, Ugo Francesco Settimio,
973 Benedetto Caroleo, Bruno Amato, Luca Gallelli, and Stefano De Franciscis. 2015.
974 “Chronic Wound Infections: The Role of Pseudomonas Aeruginosa and Staphylococcus
975 Aureus.” *Expert Review of Anti-Infective Therapy* 13 (5): 605–13.
976 https://doi.org/10.1586/14787210.2015.1023291.
977 Shopsin, Bo, Alex Drlica-Wagner, Barun Mathema, Rajan P. Adhikari, Barry N. Kreiswirth,
978 and Richard P. Novick. 2008. “Prevalence of Agr Dysfunction among Colonizing

979 Staphylococcus Aureus Strains." *Journal of Infectious Diseases* 198 (8): 1171–74.
980 https://doi.org/10.1086/592051.
981 Soberón-Chávez, Gloria, François Lépine, and Eric Déziel. 2005. "Production of
982 Rhamnolipids by Pseudomonas Aeruginosa." *Applied Microbiology and Biotechnology*
983 68 (6): 718–25. https://doi.org/10.1007/s00253-005-0150-3.
984 Tan, Timothy L., Michael M. Kheir, Dean D. Tan, and Javad Parvizi. 2016. "Polymicrobial
985 Periprosthetic Joint Infections: Outcome of Treatment and Identification of Risk Factors."
986 *The Journal of Bone and Joint Surgery* 98 (24): 2082–88.
987 https://doi.org/10.2106/jbjs.15.01450.
988 Tognon, Mikaël, Thilo Köhler, Bartosz G. Gdaniec, Youai Hao, Joseph S. Lam, Marie
989 Beaume, Alexandre Luscher, Angus Buckling, and Christian Van Delden. 2017. "Co-
990 Evolution with Staphylococcus Aureus Leads to Lipopolysaccharide Alterations in
991 Pseudomonas Aeruginosa." *ISME Journal* 11 (10): 2233–43.
992 https://doi.org/10.1038/ismej.2017.83.
993 Tognon, Mikaël, Thilo Köhler, Alexandre Luscher, and Christian Van Delden. 2019.
994 "Transcriptional Profiling of Pseudomonas Aeruginosa and Staphylococcus Aureus
995 during in Vitro Co-Culture." *BMC Genomics* 20 (1): 1–15.
996 https://doi.org/10.1186/s12864-018-5398-y.
997 Toyofuku, Masanori, Toshiaki Nakajima-Kambe, Hiroo Uchiyama, and Nobuhiko Nomura.
998 2010. "The Effect of a Cell-to-Cell Communication Molecule, Pseudomonas Quinolone
999 Signal (PQS), Produced by P. Aeruginosa on Other Bacterial Species." *Microbes and*
1000 *Environments* 25 (1): 1–7. https://doi.org/10.1264/jsme2.ME09156.
1001 Traber, Katrina E., Elsie Lee, Sarah Benon, Rebecca Corrigan, Mariela Cantera, Bo Shopsin,
1002 and Richard P. Novick. 2008. "Agr Function in Clinical Staphylococcus Aureus Isolates."
1003 *Microbiology* 154 (8): 2265–74. https://doi.org/10.1099/mic.0.2007/011874-0.
1004 Tuchscherr, Lorena, Eva Medina, Muzaffar Hussain, Wolfgang Völker, Vanessa Heitmann,
1005 Silke Niemann, Dirk Holzinger, et al. 2011. "Staphylococcus Aureus Phenotype
1006 Switching: An Effective Bacterial Strategy to Escape Host Immune Response and

1007 Establish a Chronic Infection." *EMBO Molecular Medicine* 3 (3): 129–41.
1008 https://doi.org/10.1002/emmm.201000115.
1009 Xue, Lijun, Yang Yizhi Chen, Zhiyun Yan, Wei Lu, Dong Wan, and Huifeng Zhu. 2019.
1010 "Staphyloxanthin: A Potential Target for Antivirulence Therapy." *Infection and Drug*
1011 *Resistance* 12: 2151–60. https://doi.org/10.2147/IDR.S193649.
1012 Yung, Deborah Bow Yue, Kathleen Jean Sircombe, and Daniel Pletzer. 2021. " Friends or
1013 Enemies? The Complicated Relationship between Pseudomonas Aeruginosa and
1014 Staphylococcus Aureus ." *Molecular Microbiology*, no. October 2020: 1–15.
1015 https://doi.org/10.1111/mmi.14699.
1016 Zeden, Merve S., Orlà Burke, Moya Vallely, Claire Fingleton, and James P. O'Gara. 2021.
1017 "Exploring Amino Acid and Peptide Transporters as Therapeutic Targets to Attenuate
1018 Virulence and Antibiotic Resistance in Staphylococcus Aureus." *PLoS Pathogens*, 1–5.
1019 https://doi.org/10.1371/journal.ppat.1009093.
1020 Zeden, Merve S., Igor Kviatkovski, Christopher F. Schuster, Vinai C. Thomas, Paul D. Fey,
1021 and Angelika Gründling. 2020. "Identification of the Main Glutamine and Glutamate
1022 Transporters in Staphylococcus Aureus and Their Impact on C-Di-AMP Production."
1023 *Molecular Microbiology* 113 (6): 1085–1100. https://doi.org/10.1111/mmi.14479.
1024